

A New Fluorescent Probe for Zinc(II): An 8-Hydroxy-5-*N,N*-dimethylaminosulfonylquinoline-Pendant 1,4,7,10-Tetraazacyclododecane

Shin Aoki,^{*,[a, b]} Kazusa Sakurama,^[c] Nanako Matsuo,^[a] Yasuyuki Yamada,^[a, b] Ryoko Takasawa,^[d] Sei-ichi Tanuma,^[a, d] Motoo Shiro,^[e] Kei Takeda,^[c] and Eiichi Kimura^[f]

Abstract: A new fluorescent probe for Zn²⁺, namely, 8-hydroxy-5-*N,N*-dimethylaminosulfonylquinolin-2-ylmethylpendant cyclen (L⁸), was designed and synthesized (cyclen = 1,4,7,10-tetraazacyclododecane). By potentiometric pH, ¹H NMR, and UV spectroscopic titrations, the deprotonation constants p*K*_{a1}–p*K*_{a6} of L⁸·4HCl were determined to be <2, <2, <2 (for amino groups of the cyclen and quinoline moieties), 7.19 ± 0.05 (for 8-OH of the quinoline moiety), 10.10 ± 0.05, and 11.49 ± 0.05, respectively, at 25 °C with *I* = 0.1 (NaNO₃). The results of ¹H NMR, potentiometric pH, and UV titrations, as well as single-crystal X-ray diffraction

analysis, showed that L⁸ and Zn²⁺ form a 1:1 complex [Zn(H₋₁L⁸)], in which the 8-OH group of the quinoline ring of L⁸ is deprotonated and coordinates to Zn²⁺, in aqueous solution at neutral pH. On addition of one equivalent of Zn²⁺ and Cd²⁺, the fluorescence emission of L⁸ (5 μM) at 512 nm in aqueous solution at pH 7.4 [10 mM HEPES with *I* = 0.1 (NaNO₃)] and 25 °C increased by factors of 17 and 43, respectively. We found that the cyclen moiety has

the unique property of quenching the fluorescence emission of the quinolinol moiety when not complexed with metal cations, but enhancing emission when complexed with Zn²⁺ or Cd²⁺. In addition, the Zn²⁺–L⁸ complex [Zn(H₋₁L⁸)] is much more thermodynamically and kinetically stable (*K*_d{Zn(H₋₁L⁸)} = [Zn²⁺]_{free}[L⁸]_{free}/[Zn(H₋₁L⁸)] = 8 fM at pH 7.4) than the Zn²⁺ complexes of our previous Zn²⁺ fluorophores ([Zn(H₋₁L²)] and [Zn(L³)]). Furthermore, formation of [Zn(H₋₁L⁸)] is much faster than those of [Zn(H₋₁L²)] and [Zn(L³)]. The staining of early-stage apoptotic cells with L⁸ is also described.

Keywords: bioinorganic chemistry • fluorescent probes • host–guest systems • macrocyclic ligands • zinc

Introduction

Zinc(II) is the second most abundant transition metal after iron and an essential element in natural biological systems.^[1] Most Zn²⁺ is found as a catalytic or cocatalytic factor in the active sites of more than 300 enzymes including carbonic an-

hydrase, carboxypeptidase, class II aldolase, alkaline phosphatase, and collagenase,^[2] and as a structural factor in many enzymes or proteins, such as zinc finger peptides.^[3] Zn²⁺ apparently plays important physiological roles in living systems as a neural signal transmitter^[4] and an allosteric regulator of G protein-coupled receptors (GPCR) such as β₂

[a] Prof. S. Aoki, N. Matsuo, Dr. Y. Yamada, Prof. S.-i. Tanuma
Faculty of Pharmaceutical Sciences, Tokyo University of Science
2641 Yamazaki, Noda 278-8510 (Japan)
Fax: (+81)4-7121-3670
E-mail: shinaoki@rs.noda.tus.ac.jp


[b] Prof. S. Aoki, Dr. Y. Yamada
Center for Drug Delivery Research
Faculty of Pharmaceutical Sciences, Tokyo University of Science
2641 Yamazaki, Noda 278-8510 (Japan)

[c] K. Sakurama, Prof. K. Takeda
Division of Medicinal Chemistry
Graduate School of Biomedical Sciences, Hiroshima University
1-2-3 Kasumi, Minami-ku, Hiroshima, 734-8551 (Japan)

[d] Dr. R. Takasawa, Prof. S.-i. Tanuma
Genome and Drug Research Center, Tokyo University of Science
2641 Yamazaki, Noda 278-8510 (Japan)

[e] Dr. M. Shiro
Rigaku Corporation X-ray Research Laboratory
3-9-12 Matsubaracho, Akishima, Tokyo, 196-8666 (Japan)

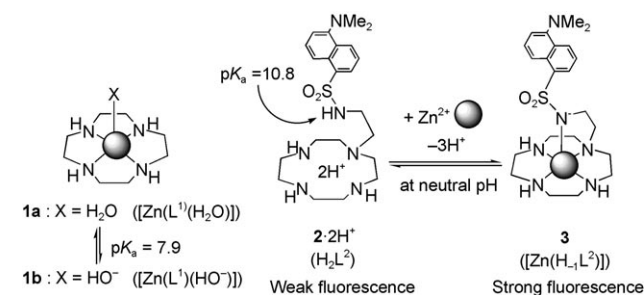
[f] Prof. E. Kimura
Faculty of Integrated Arts and Sciences, Hiroshima University
1-7-1 Kagamiyama, Higashi-Hiroshima, 739-8521 (Japan)

 Supporting information for this article is available on the WWW under <http://www.chemeurj.org/> or from the author.

adrenergic receptors or dopamine D₂ receptors.^[5] In addition, Zn²⁺ is reported to be a key intracellular regulator of apoptosis, that is, programmed cell death occurring during embryogenesis, lymphocyte selection in the thymus, immunological responses, and many other physiological and pathological situations.^[6] It is now assumed that an intracellular pool contains Zn²⁺ (free or loosely bound) in the micromolar to picomolar range.^[7]

To elucidate the biological roles of Zn²⁺, which is spectroscopically silent due to its d¹⁰ electron configuration, the demand for determining the concentration of Zn²⁺ in sample solutions and in living cells is growing rapidly.^[8] Up to now, Zn²⁺-selective fluorescent sensors including 6-methoxy-8-*p*-toluenesulfonamidoquinoline (TSQ), 6-methoxy-8-*p*-toluenesulfonamidoquinoline (2-Me-TSQ), and Zinquin have been developed, the fluorescence of which is enhanced considerably on complexation with Zn²⁺.^[9,10] Zinquin is an effective apoptosis sensor by detecting free Zn²⁺ in apoptotic cells at early stages.^[10] Since the discovery of TSQ and Zinquin, the design and synthesis of many Zn²⁺ fluorophores have been reported, and some of them have been used for the detection of Zn²⁺ in cultured cells.^[11–14]

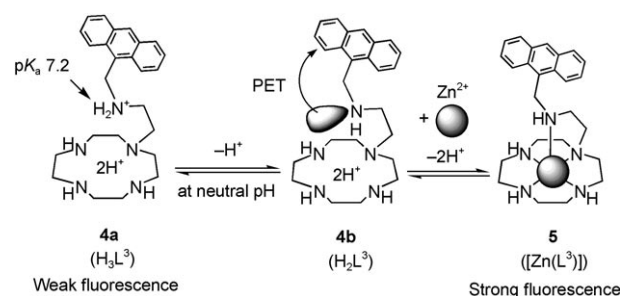
Macrocyclic polyamines such as 1,4,7,10-tetraazacyclododecane (cyclen) form very stable Zn²⁺ complexes such as [Zn²⁺(cyclen)] (**1**, [Zn(L¹)]) in aqueous solution at neutral pH (Scheme 1).^[15,16] Therefore, cyclen is a promising and



Scheme 1.

suitable chelator for Zn²⁺ fluorophores. We previously reported that dansylamide-*p*-pendant cyclen **2** (L²) quantitatively responds to Zn²⁺ at submicromolar concentrations in aqueous solution as a result of dansylamide deprotonation in 1:1 complex **3** ([Zn(H₋₁L²)]; Scheme 1), the dissociation constant of which $K_d\{\mathbf{3}\}$, was about 8 μM at pH 7.4.^[17,18] We also reported that **2** is a more stable indicator of apoptosis than Zinquin^[9,10] and acts alone to detect early-stage apoptotic cells.^[19]

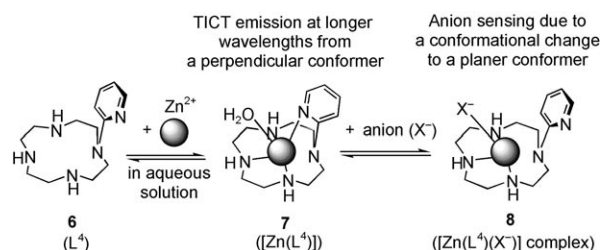
To improve Zn²⁺ selectivity and sensitivity, (anthrylmethylamino)ethyl cyclen **4** (L³) was synthesized (Scheme 2).^[20] The emission enhancement in the 1:1 Zn²⁺-L³ complex **5** ([Zn(L³)]) is due to the retardation of photoinduced electron transfer (PET) by chelation of a nitrogen atom of the side chain to Zn²⁺. Interestingly, **5** is more stable than **3** at a slightly acidic pH (see below), possibly because of the lower p*K*_a value (7.2) of the ammonium proton of the side chain



Scheme 2.

(for **4a** ⇌ **4b** + H⁺) than the p*K*_a (10.8) of the sulfonamide proton of **2** (Scheme 1).^[17,20]

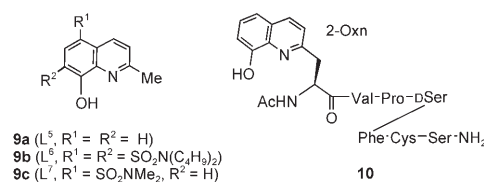
Recently, we reported a new Zn²⁺ fluorophore based on the chelation-controlled twisted intramolecular charge transfer (TICT) utilizing the simple ligand 2-pyridylcyclen (**6**, L⁴, Scheme 3).^[21] In the absence of Zn²⁺, the emission maxi-



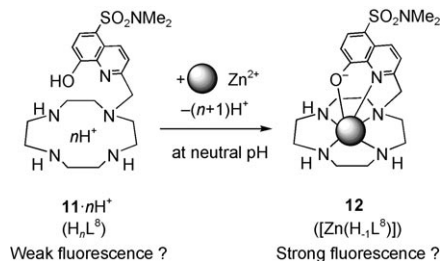
Scheme 3.

mum of **6** was observed at 356 nm at neutral pH. On complexation with Zn²⁺, the pyridyl nitrogen atom of L⁴ chelates to Zn²⁺ in 1:1 complex **7** ([Zn(L⁴)]) to fix a perpendicular conformation of the pyridine ring with respect to the dialkylamino group in the 2-position, and the emission shifts to 430 nm from the TICT state. Furthermore, it was found that anion (X⁻) coordination to Zn²⁺ of **7** yields [Zn(L⁴)X⁻] complex **8**, the emission of which shifts to about 350 nm and allows anion sensing.

8-Hydroxyquinoline (**9a**, 8-HQ, also called oxine) and its derivatives such as **9b** (L⁶) and **9c** (L⁷) are classified in the second most important category of chelating agents after EDTA and are used as fluorescence sensors of various metal cations.^[8b,22] While 8-HQ generally does not exhibit good selectivity for specific metal ions, a hexapeptide **10** containing a Val-Pro-D-Ser-Phe-Cys-Ser sequence (for reverse-turn formation) with an artificial amino acid having an 8-HQ unit (2-Oxn), designed by Imperiali et al., was shown to exhibit Zn²⁺ selectivity.^[23] Later, they examined the fluorescence response of 8-HQ derivatives **9a–c** to Zn²⁺.^[24]



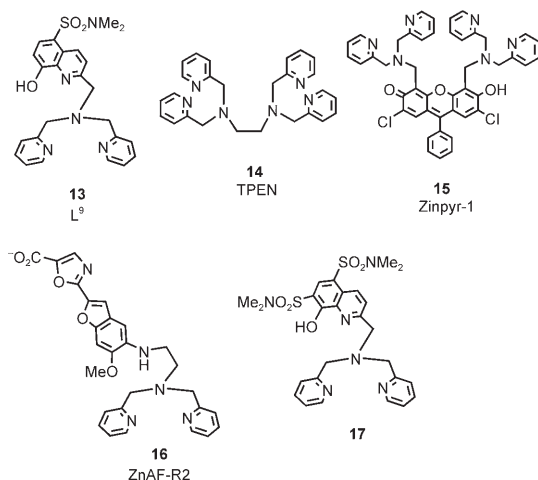
At 500 nm, the fluorescence emissions of **9a** and **9c** (**9a** or **9c**] = 5 μM) increase by a factor of 8–15 on addition of ten equivalents of Zn²⁺ in 10:90 CH₃CN/10 mM HEPES [pH 7.4 with *I* = 0.1 (NaNO₃)] at 25 °C (see below). We have thus designed and synthesized new cyclen-based Zn²⁺ fluorophore **11** (L⁸) having an 8-hydroxy-5-*N,N*-dimethylaminosulfonyl-



Scheme 4.

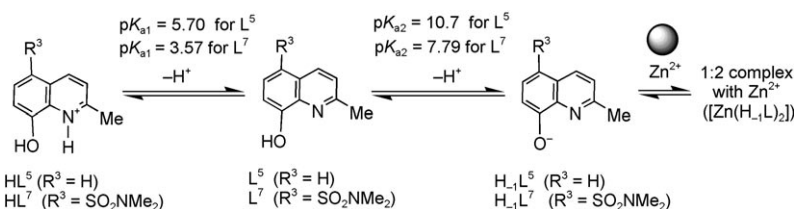
quinoline unit on the side chain (Scheme 4). We postulated that **11** would form a 1:1 complex [Zn(H₈L⁸)] (**12**), in which deprotonation of the hydroxyl group of 8-HQ and chelation to Zn²⁺ at neutral pH allow more sensitive detection of Zn²⁺ than **2** and **4**. Herein we describe potent Zn²⁺ complexation by **11** and quantitative Zn²⁺ sensing in aqueous solution.

In addition, we synthesized reference compound **13** (L⁹) having a di-2-picolylamine (DPA) moiety in order to compare its fluorescence properties with those of **11**. The DPA unit has been widely used for potent Zn²⁺ chelators such as *N,N,N',N'*-tetrakis(2-pyridylmethyl)ethylenediamine (TPEN, **14**),^[7c] Zn²⁺ fluorophores including the Zinpyr series^[11] [e.g., Zinpyr-1 (**15**)],^[11a-c] the ZnAF series^[12] [e.g., ZnAF-R2 (**16**)],^[12d] and **17**.^[13b]



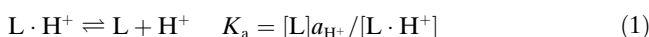
Results and Discussion

Deprotonation and fluorescence behavior of 8-hydroxy-2-methylquinoline derivatives: Prior to the synthesis of the new ligands, we conducted potentiometric pH titrations of 8-hydroxy-2-methylquinoline (**9a**) and 8-hydroxy-2-methyl-5-*N,N*-dimethylaminosulfonylquinoline (**9c**)^[24] with *I* = 0.1 (NaNO₃) at 25 °C and calculated their p*K*_a values, defined by Equation (1), by using the program BEST.^[25] As summarized in Scheme 5, p*K*_a values for L⁵ of 3.57 (p*K*_{a1}) and 7.79 (p*K*_{a2}) were lower than those for L⁵ of 5.70 (p*K*_{a1}) and 10.7 (p*K*_{a2}), due to the electron-withdrawing effects of the *N,N*-dimethylaminosulfonyl group at the 5-position. The results of UV titrations of **9a** and **9c** (**9a** or **9c**] = 50 μM) with Zn²⁺ in 99:1 EtOH/10 mM HEPES [pH 7.4 with *I* = 0.1 (NaNO₃)] at 25 °C (Supporting Information) strongly suggest 2:1 complexation of **9a** or **9c** with Zn²⁺. Fluorescence titration of

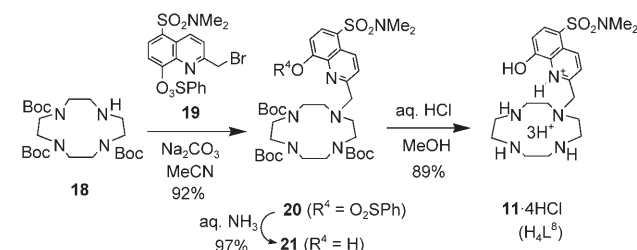


Scheme 5.

9a and **9c** (5 μM) with Zn²⁺ in 10/90 CH₃CN/10 mM HEPES [pH 7.4 with *I* = 0.1 (NaNO₃)] at 25 °C showed that the emissions of **9a** and **9c** increase by a factor of 8–15 on addition of ten equivalents of Zn²⁺ (excitation at 334–335 nm), as shown in the Supporting Information (the quantum yield Φ of **9c** increased from 4.0×10^{-3} to 1.6×10^{-1}). These data indicated that Zn²⁺ complexes of **9a** or **9c** are not so stable.



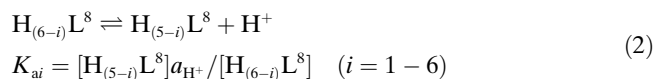
Synthesis of 11 (L⁸) and 13 (L⁹): The new ligand (8-hydroxy-5-*N,N*-dimethylaminosulfonylquinoline-pendant cyclen **11** (L⁸) was synthesized as shown in Scheme 6. Reaction of 2-bromomethyl-8-benzensulfonyloxy-5-*N,N*-dimethylaminosulfonylquinoline (**19**) with (Boc)₃cyclen **18**^[26] gave **20**, the PhSO₂ group of which was deprotected with aqueous NH₃ to afford **21**. The Boc groups of **21** were removed with aque-



Scheme 6.

ous HCl to yield **11** (L^8) as $L^8 \cdot 4HCl$. Reaction of **19** with di-2-picolyamine and successive removal of $PhSO_2$ and Boc groups gave reference compound **13** (L^9), which was isolated as $13 \cdot 4HCl$.^[27]

Deprotonation constants of **11 (L^8) determined by potentiometric pH and 1H NMR titrations:** Typical potentiometric pH titration curves (Figure 1) of a mixture of 1 mM $L^8 \cdot 4HCl + 1$ mM HNO_3 with $I = 0.1$ (NaNO₃) by addition of 0.1 M NaOH at 25 °C were analyzed for acid–base equilibrium [Eq. (2)]. The deprotonation constants pK_{ai} ($i = 1-6$) of $L^8 \cdot 4HCl$ were determined to be < 2 (pK_{a1}), < 2 (pK_{a2}), < 2 (pK_{a2}), 7.19 ± 0.05 (pK_{a4}), 10.10 ± 0.05 (pK_{a5}), and 11.49 ± 0.05 (pK_{a6}) by using the program BEST (Table 1).^[25] The pK_{a1} , pK_{a2} , pK_{a5} , and pK_{a6} values were assigned to deprotonation constants of three secondary amines in a cyclen ring by comparison with the pK_a values for cyclen (L^1),^[28] **2** (L^2),^[17] and **4** (L^3)^[20] (Table 1).



Considerable change of the 1H NMR signal for H7 of the quinoline ring of **11** (for numbering, see Scheme 7) in the

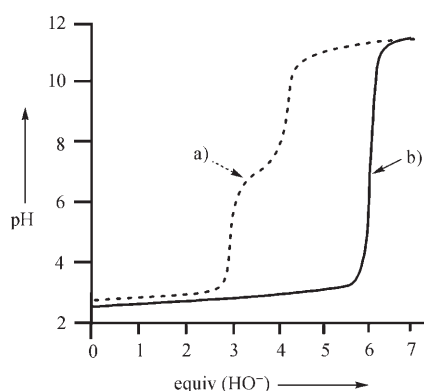
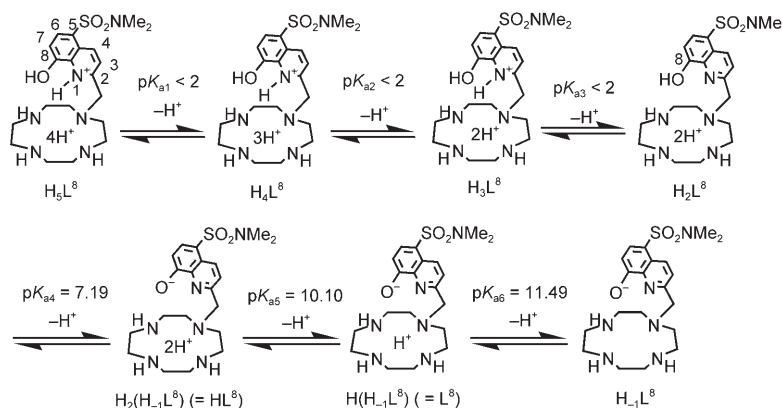


Figure 1. Typical potentiometric pH titration curves for a mixture of 1 mM $H_4L^8 + 1$ mM HNO_3 (a) and a mixture of 1 mM $H_4L^8 + 1$ mM $HNO_3 + 1$ mM Zn^{2+} (b) with $I = 0.1$ (NaNO₃) at 25 °C. Equiv(HO^-) is the number of equivalents of base (NaOH) added.

Table 1. Deprotonation constants K_{ai} and complexation constants of cyclen (L^1), **2** (L^2), **4** (L^3), and **11** (L^8) with $I = 0.1$ (NaNO₃) at 25 °C.^[a]

	Cyclen (L^1) ^[b]	2 (L^2) ^[c]	4 (L^3) ^[d]	11 (L^8)
pK_{a1}	< 2	< 2	< 2	< 2
pK_{a2}	< 2	2.2	< 2	< 2
pK_{a3}	9.9	4.0	7.2	< 2
pK_{a4}	11.0	9.4	9.1	7.19 ± 0.05 7.0 ± 0.2 ^[e]
pK_{a5}		10.8	10.6	10.10 ± 0.05
pK_{a6}		11.8		11.49 ± 0.05
$\log K_s([Zn(L)])$	16.2	20.8	17.6	22.4 ± 0.1
$\log K_{app}([Zn(L)])$ ^[f] at pH 7.4	10.6	11.1	10.7	14.1
$\log K_{app}([Zn(L)])$ ^[g] at pH 5.0	5.5	4.0	6.0	10.8 ± 0.1

[a] For the definition of $K_s([Zn(L)])$, $K_{app}([Zn(L)])$, and $pK_a([Zn(L)])$, see text. [b] From reference [28]. [c] From reference [17a]. [d] From reference [20]. [e] The pK_{a4} value was determined based on pH–UV absorption profiles (see Figure 3a and c). [f] Apparent complexation constants at pH 7.4 with $I = 0.1$ (NaNO₃). [g] Apparent complexation constants at pH 5.0 with $I = 0.1$ (NaNO₃).



Scheme 7.

pD range of 5.5–8.5 in D₂O (Supporting Information) implies that the pK_a value for the 8-OH group of **11** is 7.2 ± 0.2 . This value agrees well with the pK_a value (7.0) obtained from its pH–UV profile (see below).

The structure of the $H_2(H_{1-1}L^8)$ ($=HL^8$) form was confirmed by single-crystal X-ray diffraction analysis of a fine colorless prism of **11** obtained from an aqueous solution at pH 10. Figure 2 shows the hydrogen-bonding network including the deprotonated 8-OH group, an ammonium proton of the cyclen ring, four water molecules, and one Cl^- ion. Based on these results, the deprotonation behavior of L^8 is summarized in Scheme 7 and Table 1.

Because the solubility of reference ligand $13 \cdot 4HCl$ (H_4L^9) in aqueous solution was low, the pK_a value of 8-OH of **13** at 25 °C was determined by the pH-dependent 1H NMR spectral change (at $[13] = 1$ mM in 20/80 CD₃CN/D₂O, data not shown) and pH–UV profile (at $[13] = 0.1$ mM, see Figure 4) to be 7.2 ± 0.2 and 7.4 ± 0.2 , respectively.

The pH-dependent change of UV and fluorescence spectra of **11 (L^8) and **13** (L^9):** The UV spectra of **11** (L^8) in the pH range of 5–11 are shown in Figure 3a ($[11] = 50$ μ M). From the sigmoidal curve of ϵ_{258} in Figure 3c, the pK_a value for 8-OH in the ground state of **11** was determined to be 7.0 ± 0.2 , which agrees well with the pK_a values obtained from the po-

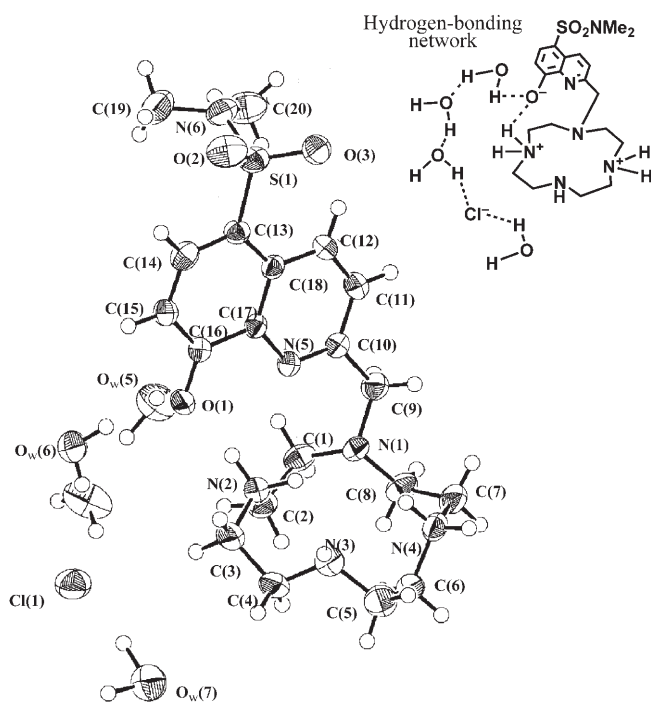


Figure 2. ORTEP drawing (50% probability ellipsoids) of **11** in the $H_2-(L^8)$ form. Selected bond lengths [Å]: S(1)–O(2) 1.4395(15), S(1)–O(3) 1.4328(14), S(1)–N(6) 1.6339(18), C(16)–O(1) 1.302(2); selected dihedral angles [°]: N(1)–C(1)–C(2)–N(2) 52.7, N(2)–C(3)–C(4)–N(3) 55.0, N(3)–C(5)–C(6)–N(4) 64.9, N(4)–C(7)–C(8)–N(1) 58.6, C(14)–C(13)–S(1)–N(6) 86.0.

tentiometric pH (7.19) and 1H NMR titrations (7.0) described above.

Figure 3b shows fluorescence emission spectra of $5 \mu M$ **11** (L^8) in the pH range of 5–12 [10 mM Good's buffer with $I=0.1$ ($NaNO_3$)] at $25^\circ C$ (excitation at 338 nm, which is an isosbestic point obtained from UV titrations; Figure 3a). As the pH is raised, emission at 478 nm increases with a sigmoidal curve giving a pK_a value of 10.0 ± 0.2 (Figure 3c), which is different from the pK_a value of 7.0–7.2 in the ground state described above. The quantum yields Φ of L^8 at pH 7.4 and 12 are 2.0×10^{-3} and 1.7×10^{-1} , respectively. This discrepancy in pK_a values is discussed below.

The pH-dependent changes in UV absorption and fluorescence emission spectra of **13** (L^9) in the pH range of 4–11 are summarized in Figure 4 ([**13**]= $50 \mu M$ for UV spectra and $5 \mu M$ for emission spectra). From the sigmoidal curve of ϵ_{261} (open circles), the pK_a value for 8-OH was determined to be 7.4 ± 0.2 , which is in fair agreement with the pK_a value of 7.2 ± 0.2 obtained from 1H NMR titrations (data not shown). The change in emission intensity of **13** at 496 nm (excitation at 338 nm) plotted in Figure 4 (filled circles) at pH 4–10 [10 mM Good's buffer with $I=0.1$ ($NaNO_3$)] and $25^\circ C$ was somewhat complex, and this hampered the estimation of the pK_a value of **13** in the excited state.^[29] For comparison, emission intensities of $5 \mu M$ **9c** (L^7) at 478 nm (filled squares in Figure 4) were very low at pH 4–11 (Φ at pH 7.4 was 1.0×10^{-3}).

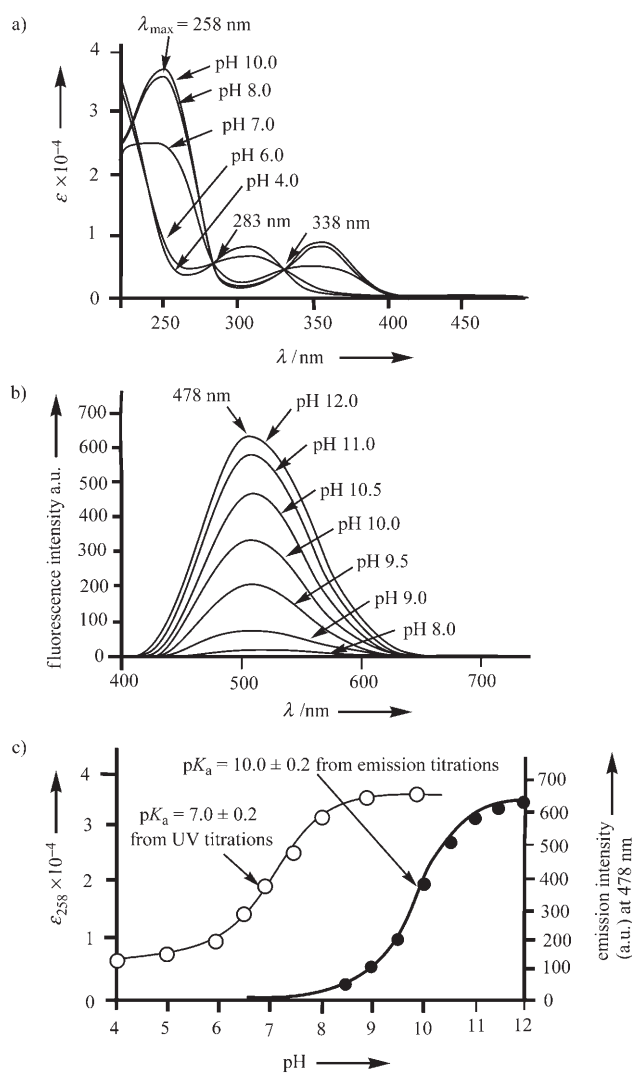


Figure 3. a) Change in UV spectra of $50 \mu M$ **11** (L^8) in the range pH 4.0–12.0 (Good's buffer) with $I=(NaNO_3)$ at $25^\circ C$. b) Change in emission spectra of $5 \mu M$ **11** (L^8) in the range pH 8.0–12.0 with $I=(NaNO_3)$ at $25^\circ C$ (excitation at 338 nm). c) Comparison of pH-dependent change in ϵ_{258} (open circles) and emission intensity at 478 nm (filled circles) of $5 \mu M$ **11** (L^8) with $I=0.1$ ($NaNO_3$) at $25^\circ C$.

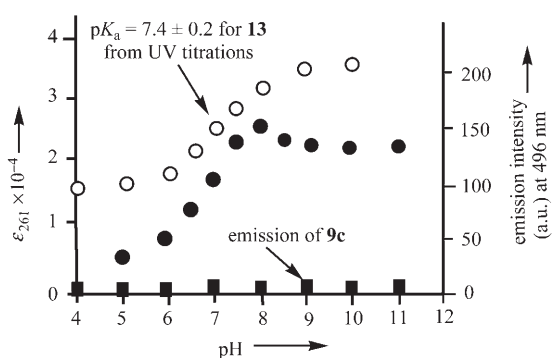
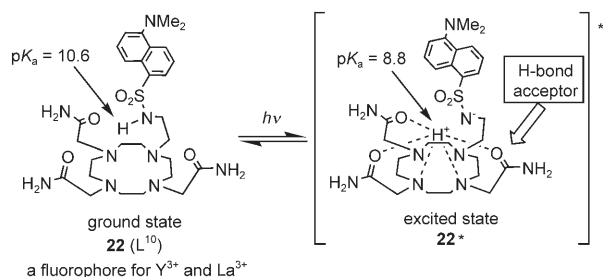


Figure 4. Comparison of pH-dependent change in ϵ_{261} (open circles) and emission intensity at 496 nm (filled circles) of **13** (L^9) with $I=0.1$ ($NaNO_3$) at $25^\circ C$ (excitation at 338 nm; [**13**]= $50 \mu M$ for UV spectra and $5 \mu M$ for emission spectra). Filled squares indicate emission intensity of $5 \mu M$ **9c** (L^7) at 496 nm (excitation at 338 nm).

Discrepancy of the pK_a values for the 8-OH group of **12 (L^8) determined by pH-UV and pH-emission profiles:** It was unexpected that the pK_a value of 10.0 for 8-OH-quinoline of **11** (L^8) in the excited state as determined by pH-emission profile (Figure 3c) would be different from the pK_{a3} value for the 8-OH group in the ground state of 7.2 determined by potentiometric pH titrations and pH-dependent UV spectra.

With regard to this kind of discrepancy of the pK_a values between ground and excited states, we previously reported a selective fluorescent probe for La^{3+} and Y^{3+} , namely, **22** (L^{10}), which has a dansyl group and three carbamoyl groups as side chains (Scheme 8).^[30] The pK_a value of the dansyl-

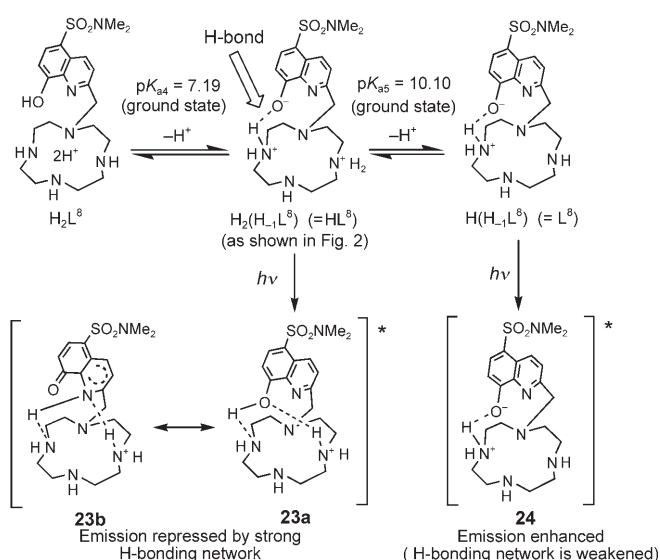


Scheme 8.

amide proton of metal-free **22** in the ground state (determined by potentiometric pH and UV titrations) was 10.6, which differed from the pK_a value of 8.8 for the same proton in the excited state (obtained by pH-emission profile). We concluded that the dansylamide-deprotonated form of **22** is stabilized by hydrogen bonds between the dansylamide proton and the carbamoyl groups (hydrogen-bond acceptors) in the excited state **22***, which result in increased fluorescence emission above pH 8–9.

The structure of $H_2(H_{-1}L^8)$ ($=HL^8$) was confirmed by single-crystal X-ray diffraction analysis (Figure 2 and Scheme 9). By analogy with the photochemical properties of **22** (L^{10}), we postulated that the neutral forms of the 8-OH-quinoline moiety in $H_2(H_{-1}L^8)$ in the excited state (**23a** and/or its tautomer **23b**^[31] in Scheme 9) are stabilized by a hydrogen-bonding network formed by the 8-OH group and two ammonium cations of cyclen, which results in repression of the fluorescent emission of **11** below pH 8. We assume that further deprotonation of the cyclen ring in $H_2(H_{-1}L^8)$, which gives $H(H_{-1}L^8)$ ($=L^8$), weakens the hydrogen-bonded network and enhances emission from the excited state of L^8 (**24** in Scheme 9).

UV and fluorescence titrations of **11 (L^8) and **13** (L^9) with Zn^{2+} :** Figure 5a shows the results of UV absorption titrations of 0.1 mM **11** (L^8) with Zn^{2+} at pH 7.0 [10 mM HEPES with $I=0.1$ ($NaNO_3$)] and 25 °C with isobestic points at 268 and 338 nm. The inset shows the linear increase in ϵ_{258} ($\epsilon_{258} = 2.5 \times 10^{-4}$ for metal-free **11**) with increasing concentrations of Zn^{2+} .



Scheme 9.

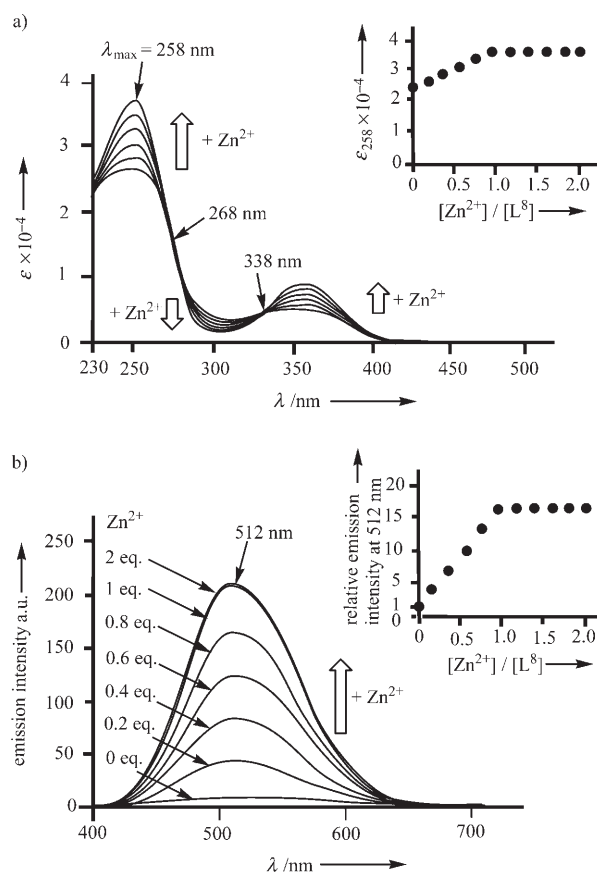


Figure 5. a) Change in UV absorption spectra of 0.1 mM **11** (L^8) on addition of Zn^{2+} at pH 7.4 [10 mM HEPES with $I=0.1$ ($NaNO_3$)] and 25 °C. The inset shows the titration curve (increasing ϵ_{258}) of **11** with Zn^{2+} at pH 7.4 [10 mM HEPES with $I=0.1$ ($NaNO_3$)] and 25 °C. b) Change in emission spectra of 5 μ M **11** (L^8) on addition of Zn^{2+} at pH 7.0 [10 mM HEPES with $I=0.1$ ($NaNO_3$)] and 25 °C (excitation at 338 nm). The inset shows the increase in the relative emission intensity (I/I_0) of **11** at 512 nm on addition of Zn^{2+} at pH 7.4 [10 mM HEPES with $I=0.1$ ($NaNO_3$)] and 25 °C, in which I_0 = emission intensity of L^8 at 512 nm in the absence of Zn^{2+} .

The emission of metal-free **11** ($5 \mu\text{M}$) was very weak at pH 7.4 (excitation at 338 nm) as described above (Figure 3b), and it quantitatively increased on addition of Zn^{2+} and reached a plateau at $[\mathbf{11}] = [\text{Zn}^{2+}] = 5 \mu\text{M}$ (Figure 5b), which is a strong indication for 1:1 complexation of **11** with Zn^{2+} . As shown in the inset, the emission of **11** at 512 nm increased by about 17 times with increasing $[\text{Zn}^{2+}]$ (Φ of **11** increased from 2.0×10^{-3} to 4.4×10^{-2}). The 1:1 complexation of **11** with Zn^{2+} was also confirmed by ^1H NMR titrations (Supporting Information).

The results of UV titrations of the reference compound **13** (L^9) (0.1 mM) with Zn^{2+} at 7.4 [10 mM HEPES with $I = 0.1$ (NaNO_3)] were similar to those of **11** (L^8), as shown in Figure 6A. The increase in absorption at 261 nm and the inset of Figure 6a imply quantitative formation of the 1:1 complex $[\text{Zn}(\text{H}_{-1}\text{L}^9)]$ with deprotonation of the 8-OH group of the quinoline moiety. In contrast, addition of Zn^{2+} to **13** ($5 \mu\text{M}$) induced a linear decrease in its fluorescence emission at 496 nm (excitation at 338 nm), as shown in Figure 6b and

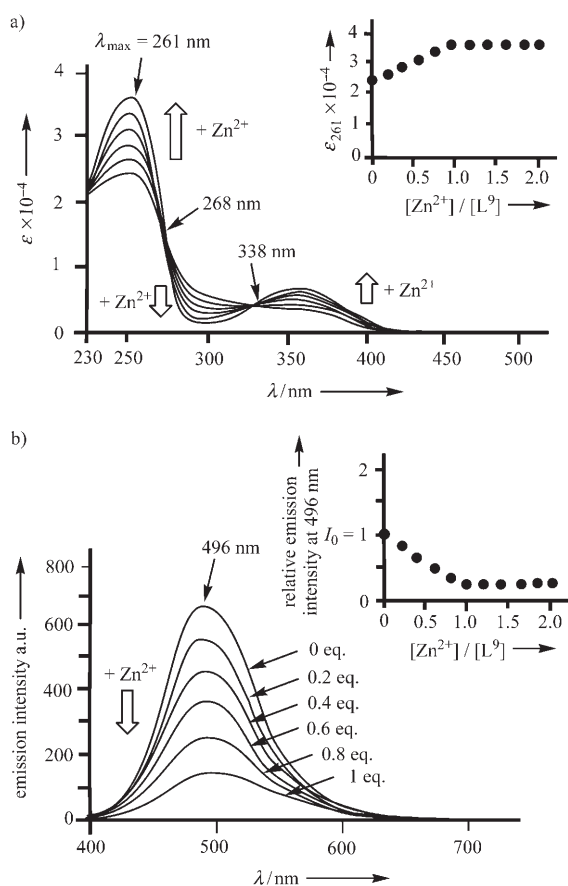


Figure 6. a) Change in UV absorption spectra of 0.1 mM **13** (L^9) on addition of Zn^{2+} at pH 7.4 [10 mM HEPES with $I = 0.1$ (NaNO_3)] and 25 °C. The inset shows the titration curve (increasing ϵ_{261}) of **13** with Zn^{2+} at pH 7.4 [10 mM HEPES with $I = 0.1$ (NaNO_3)] and 25 °C. b) Change in fluorescence emission of 5 μM **13** upon addition of Zn^{2+} at pH 7.4 [10 mM HEPES with $I = 0.1$ (NaNO_3)] and 25 °C (excitation at 338 nm). The inset shows the change in emission intensity (I/I_0) of **13** at 496 nm on addition of Zn^{2+} at pH 7.4 [10 mM HEPES with $I = 0.1$ (NaNO_3)] and 25 °C, in which I_0 = emission intensity of the metal-free L^9 at 496 nm.

its inset (Φ decreased from 6.1×10^{-2} to 2.1×10^{-2}), presumably because metal-free **13** had its own moderate emission.^[32]

X-ray crystal structure of $[\text{Zn}(\text{H}_{-1}\text{L}^8)]$ complex **12:** Fine colorless crystals were obtained from a 1:1 mixture of **11** (L^8) and Zn^{2+} in aqueous solution at pH 7.0. Single-crystal X-ray structure analysis disclosed that Zn^{2+} in the $[\text{Zn}(\text{H}_{-1}\text{L}^8)]$ complex **12** is sixfold-coordinated by deprotonated O(1) at the 8-position of the quinoline ring, N(5) of the quinoline ring, and N(1)–N(4) of the cyclen ring (Figure 7). The of Zn^{2+} –O(1) and Zn^{2+} –N(5) bond lengths of 2.10 and 2.09 Å, respectively, are shorter than the average Zn^{2+} –N(cyclen) distance of 2.21 Å. Four N atoms of the cyclen ring and the Zn^{2+} ion form a tetragonal-pyramidal structure.

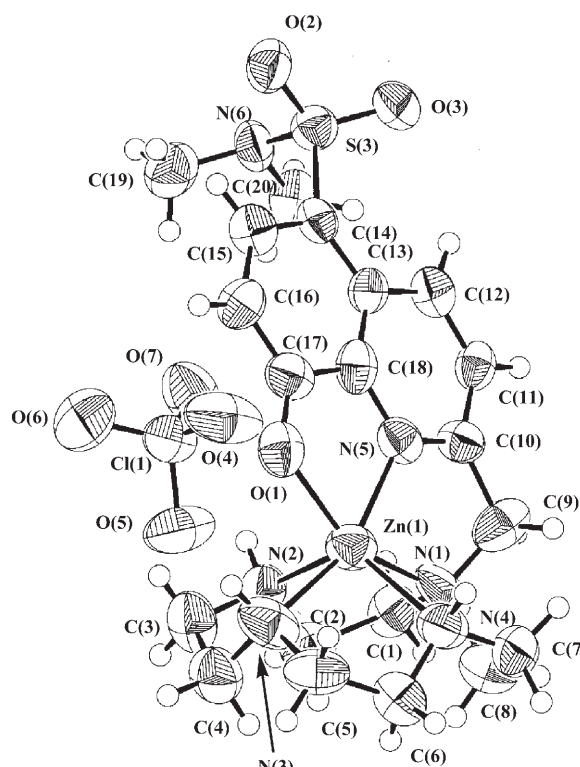


Figure 7. ORTEP drawing (50% probability ellipsoids) of $[\text{Zn}(\text{H}_{-1}\text{L}^8)]$ (**12**). Selected bond lengths [Å]: Zn(1)–O(1) 2.095(8), Zn(1)–N(1) 2.30(1), Zn(1)–N(2) 2.162(1), Zn(1)–N(3) 2.18(1), Zn(1)–N(4) 2.180(8), Zn(1)–N(5) 2.094(9).

Comparison of fluorescence responses of **2 (L^2), **4** (L^3), **11** (L^8), and **13** (L^9) to Zn^{2+} , Cd^{2+} , and Cu^{2+} :** Fluorescence responses of 5 μM **11** (L^8) to Zn^{2+} , Cd^{2+} , and Cu^{2+} at pH 7.4 [10 mM HEPES with $I = 0.1$ (NaNO_3)] and 25 °C are compared with those of **2** (L^2), **4** (L^3), and **13** (L^9) in Figure 8. As previously reported,^[17] **2** and **4** (at 5 μM) responded to Zn^{2+} , which resulted in a linear increase in emission (Figure 8a and b). Addition of Cd^{2+} to **2** gave almost the same titration curve as that of Zn^{2+} .^[17] Cu^{2+} quantitatively quenched the emission of **2** and **4**.

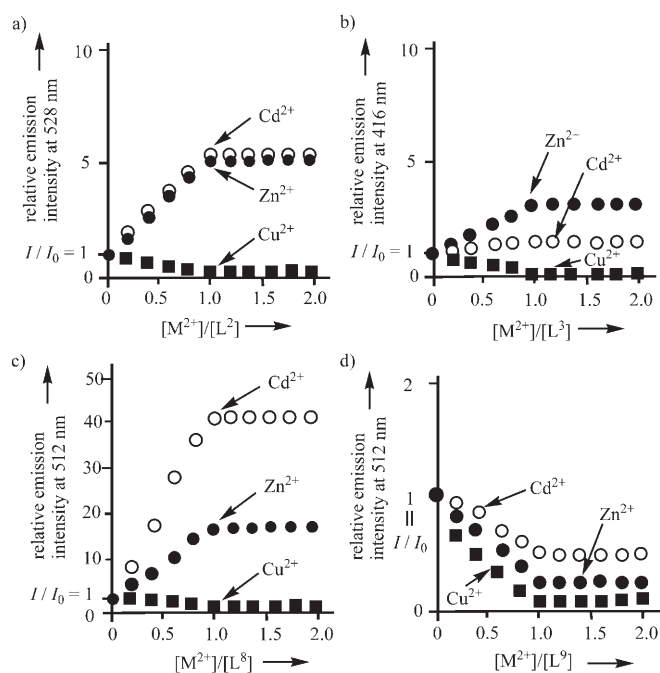
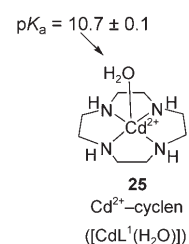


Figure 8. Comparison of fluorescent response of a) **2** (L^2) (from ref. [17a]), b) **4** (L^3) (from ref. [20]), c) **11** (L^8), and d) **13** (L^9) to Zn^{2+} , Cd^{2+} , and Cu^{2+} at pH 7.4 [20 mM HEPES with $I=0.1$ ($NaNO_3$)] and 25 °C. I_0 is the emission intensity of each ligand at the indicated wavelength (528 nm for L^2 , 416 nm for L^3 , 512 nm for L^8 and L^9). The excitation wavelengths were 330 nm for **2**, 368 nm for **4**, and 338 nm for **11** and **13**.

Figure 8c shows that **11** (L^8) linearly responds not only to Zn^{2+} (17-fold increase in emission) but also to Cd^{2+} (43-fold increase). We assume that the stronger response to Cd^{2+} is not a problem, because this metal is not present in significant amounts in biological cells. The UV titrations of **11** (L^8) with Cd^{2+} and Cu^{2+} gave almost the same results as those in Figure 5a, and this strongly suggests that the 8-OH group of **11** is deprotonated on complexation with Cd^{2+} and Cu^{2+} (data not shown). The X-ray crystal structure analysis of the $[Cu^{2+}(H_{-1}L^8)]$ complex (**30**) obtained from an aqueous solution at pH 7 revealed that Cu^{2+} is sixfold-coordinated by deprotonated O(1), the N atom of the quinolinol moiety, and the four N atoms of the cyclen ring (Supporting Information).^[33,34] In contrast, emission of reference compound **13** decreased on addition of Zn^{2+} , Cd^{2+} , and Cu^{2+} (Figure 8d). These results enabled us to conclude that **11** (L^8) is a better Zn^{2+} fluorophore than DPA-based fluorophore **13**.

Comparison of Lewis acidity of Zn^{2+} and Cd^{2+} based on pH titrations of Zn^{2+} -cyclen and Cd^{2+} -cyclen: Figure 8c showed that emission intensity at 512 nm of the Cd^{2+} complex of **11** was much larger than that of the Zn^{2+} complex of **11** (**12**). We assumed that the emission intensity of the metal complexes of **11** is dependent on the Lewis acidity of the central metal cation. Thus, we compared the pK_a value for the Cd^{2+} -bound water of Cd^{2+} -cyclen **25** (CdL^1) with that of the Zn^{2+} -bound water in Zn^{2+} -cyclen **1a**.^[28] By potentiometric

pH titrations, the pK_a of the Cd^{2+} -bound H_2O in **25** at 25 °C [with $I=0.1$ ($NaNO_3$)] was determined to be 10.7 ± 0.1 (see Supporting Information for a typical potentiometric pH titration curve for **25**), which is higher than that (7.9)^[15,28] of the Zn^{2+} -bound H_2O in **1** (see Scheme 1). Therefore, we attributed the lower emission intensity of Zn^{2+} complex $[Zn(H_{-1}L^8)]$ (**12**) relative to $[Cd(H_{-1}L^8)]$ to the higher Lewis acidity of Zn^{2+} .



Complexation behavior of **11 (L^8) with Zn^{2+} based on potentiometric pH titrations:** Analysis of a potentiometric pH titration curve for a mixture of 1 mM H_3L^8 and 1 mM $ZnSO_4$ (curve b in Figure 1) with the program BEST^[25] gave a complexation constant $\log K_s([Zn(L)])$, defined by Equation (3), for L^8 of 22.4, from which the apparent complexation constants $\log K_{app}([Zn(L)])$, defined by Equations (4) and (5), were calculated to be 14.1 and 10.8 at pH 7.4 and 5.0, respectively (dissociation constant $K_d([Zn(L)])=1/K_{app}([Zn(L)])$ at pH 7.4 is 7.9 fM). These values are much larger than those for the previous Zn^{2+} complexes $[Zn(H_{-1}L^2)]$ (**3**) and $[Zn(L^3)]$ (**5**).

$$K_s([Zn(L^8)]) = [Zn(H_{-1}L^8)]/[H_{-1}L^8][Zn^{2+}] \quad (3)$$

$$K_{app}([Zn(L^8)]) = [Zn(H_{-1}L^8)]/[L^8]_{free}[Zn^{2+}]_{free} \quad (4)$$

(at designated pH)

$$[L^8]_{free} = [H_3L^8] + [H_4L^8] + [H_3L^8] + [H_2L^8] + [H_2(H_{-1}L^8)] + [H(H_{-1}L^8)] + [H_{-1}L^8] \quad (5)$$

(at designated pH)

A distribution diagram for a mixture of **11** (L^8 , 5 μM) and Zn^{2+} (5 μM) is presented in Figure 9a with a comparison with those for a mixture of **2** (L^2 , 5 μM) and Zn^{2+} (5 μM ; Figure 9b) and for a mixture of **4** (L^3 , 5 μM) and Zn^{2+} (5 μM , Figure 9c). It is apparent that $[Zn(H_{-1}L^8)]$ (**12**) is quantitatively formed in the pH range of 5–10 at micromolar concentrations and is much more stable than $[Zn(H_{-1}L^2)]$ (**3**) and $[Zn(L^3)]$ (**5**) at pH 5–9. Indeed, the fluorescent emission of $[Zn(H_{-1}L^8)]$ (**12**) at pH 4.5–10 was almost constant.^[35] Therefore, **11** would be useful for determining $[Zn^{2+}]$ over a much wider pH range (pH 5–8) than **2** (L^2) and **4** (L^3) (the emission of **11** is silent below pH 8, as shown in Figure 3c).

Fluorescent response of **11 (L^8) and **13** (L^9) to various metal ions in aqueous solution:** Next, we examined the fluorescent response of L^8 and L^9 (5 μM) to other metal ions including Co^{2+} , Ni^{2+} , Fe^{3+} , Al^{3+} , Y^{3+} , Ca^{2+} , and Mg^{2+} at pH 7.4 [10 mM HEPES with $I=0.1$ ($NaNO_3$)] and 25 °C. The I/I_0 values (I_0 and I are the emission intensities of each ligand in the absence and presence of one equivalent of metal ions: at 528 nm for L^2 , at 416 nm for L^3 , and at 512 nm for L^8 and L^9) are presented in Figure 10. Quantitative emission

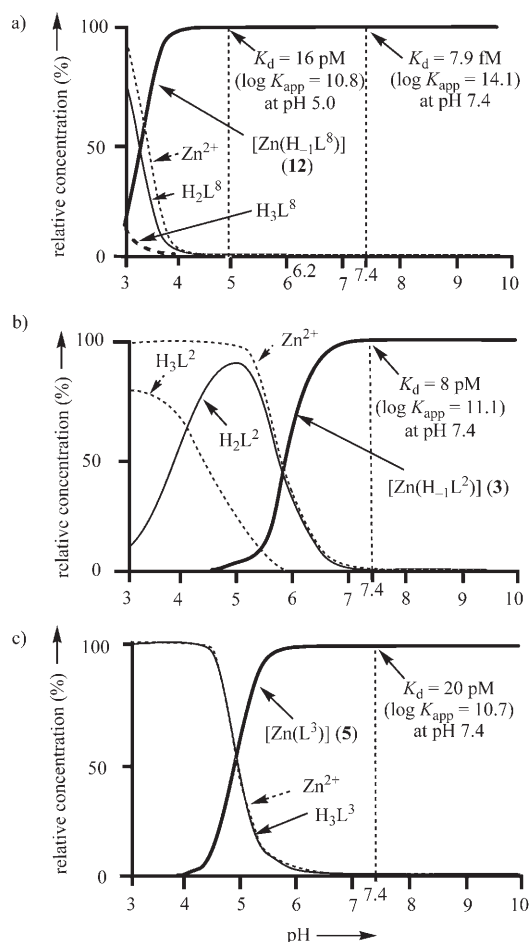


Figure 9. Distribution diagrams for a mixture of 5 μM **11** (L^8)+5 μM Zn^{2+} (a), 5 μM **2** (L^2)+5 μM Zn^{2+} (b), and 5 μM **4** (L^3)+5 μM Zn^{2+} (c) with $I=0.1$ (NaNO_3) at 25 $^\circ\text{C}$. Species of less than 10% relative concentration are omitted for clarity.

quenching was observed on addition of Cu^{2+} ; other metal ions induced negligible changes in the emission spectra of L^8 .

Kinetics of Zn^{2+} complexation of **11 (L^8) in comparison with **2** (L^2) and **4** (L^3):** The kinetics of Zn^{2+} complexation of **11** (L^8) were compared with those of our previous Zn^{2+} fluorophores **2** (L^2) and **4** (L^3) at pH 7.4 [10 mM HEPES with $I=0.1$ (NaNO_3)]. We previously reported that the second-order rate constants k_2 for formation of **3** ($[\text{Zn}(\text{H}_{-1}\text{L}^2)]$) and **5** ($[\text{Zn}(\text{L}^3)]$) are 1.4×10^2 and $4.6 \times 10^2 \text{M}^{-1}\text{s}^{-1}$, respectively, which implies that **5** is formed three times faster than **3**.^[20] These phenomena are explained by the lower $\text{p}K_a$ value of the anthrylmethylamino group ($\text{p}K_a=7.2$) of **4** (Scheme 2) compared to that (10.8) of the dansyl-amino group of **2** (Scheme 1).

Surprisingly, we found that complexation of **11** (5 μM) with Zn^{2+} and Cd^{2+} was complete within 1 min. For accurate determination of k_2 for **12**, we performed stopped-flow measurements of emission change in 10 μM **11** at pH 7.4 [10 mM HEPES with $I=0.1$ (NaNO_3)] on addition of 10, 50,

and 100 μM Zn^{2+} (Figure 11). The k_2 value for the formation of **12** ($[\text{Zn}(\text{H}_{-1}\text{L}^8)]$) was determined to be $2.1 \times 10^5 \text{M}^{-1}\text{s}^{-1}$, which is about 460 times greater than that for **5** ($[\text{Zn}(\text{L}^3)]$). The k_2 for the Zn^{2+} -**13** complex ($[\text{Zn}(\text{H}_{-1}\text{L}^9)]$) was much faster than that for **12** (k_2 for Zn^{2+} -**13** $> 1 \times 10^6 \text{M}^{-1}\text{s}^{-1}$).

Because the $\text{p}K_a$ values for **4** and **11** are almost identical (7.2), we assumed that the much larger value of k_2 for **11** is because the 8-OH group of the quinolinol moiety of **11** is fixed close to Zn^{2+} -bound water in $[\text{Zn}(\text{L}^8)(\text{H}_2\text{O})]$ (**26a**) or Zn^{2+} -bound hydroxide in $[\text{Zn}(\text{L}^8)(\text{HO}^-)]$ (**26b**) by a coordination of the quinolinol nitrogen atom to Zn^{2+} (Scheme 10). In contrast, the flexible conformation of the anthrylmethyl group of **25a** ($[\text{Zn}(\text{L}^3)(\text{H}_2\text{O})]$) or **25b** ($[\text{Zn}(\text{L}^3)(\text{HO}^-)]$) results in rather slow deprotonation of the anthrylmethylammonium moiety.

Kinetic stability of $[\text{Zn}(\text{H}_{-1}\text{L}^8)]$ complex **12:** We examined kinetic stability of $[\text{Zn}(\text{H}_{-1}\text{L}^8)]$ (**12**). The complexation constant $\log K_s$ of TPEN (**14**) with Zn^{2+} was reported to be 15.2,^[7c] which is smaller than $\log K_s$ of 22.4 for **12** (Table 1). As shown in the Supporting Information, addition of TPEN (5 μM) to a solution of **12** (5 μM) at pH 7.4 [10 mM HEPES with $I=0.1$ (NaNO_3)] caused negligible change in the emission spectra of **12** even after 3 h. Alternatively, addition of **12** (5 μM) to an aqueous solution of Zn^{2+} -TPEN complex (5 μM) under the same conditions did not enhance emission. These results strongly indicate that both $[\text{Zn}(\text{H}_{-1}\text{L}^8)]$ (**12**) and the Zn^{2+} -TPEN complex are kinetically inert.

Fluorescent staining of Zn^{2+} -loaded and apoptotic HeLaS3 cells with **11:** Incubation of HeLaS3 cells with **11** (L^8 , 50 μM) and **2** (L^2 , 50 μM) gave fluorescent images indicating that Zn^{2+} concentrations of **11** in intact HeLaS3 cells are very low (Figure 12a and b). Figure 12c and d show HeLaS3 cells incubated with Zn^{2+} (20 μM) and Zn^{2+} ionophore pyrithione (2-mercaptopyridine *N*-oxide, 200 μM) for 30 min to introduce Zn^{2+} into HeLaS3 cells and then treated with **2** and **11**, respectively. They indicate that **2** and **11** respond to Zn^{2+} transported into cells, while emissions of cells treated with **11** are less bright than those of treated with **2**,^[19] possibly because of the smaller fluorescent quantum yield ($\Phi=4.4 \times 10^{-2}$) of $[\text{Zn}(\text{H}_{-1}\text{L}^8)]$ (**12**) compared to that ($\Phi=1.1 \times 10^{-1}$) of $[\text{Zn}(\text{H}_{-1}\text{L}^2)]$ (**3**). We do not exclude the possibility that the cell-permeation of **11** is less efficient than that of **2**, due to the somewhat hydrophilic properties of the 8-quinoline group of **11**. Although incubation of HeLaS3 cells with **2** and **11** for 36 h tend to induce apoptosis, a short exposure (e.g., 1 h) did not cause significant damage to HeLaS3 cells.

Apoptosis is a mechanism of cell suicide that eliminates excess cells during development and is different from necrosis. Apoptosis includes a unique series of morphologic changes such as cell shrinkage and budding of the cell contents into membrane-enclosed vesicles (blebbing).^[36] A common method for the detection of apoptosis is visualizing DNA fragmentation in apoptotic cells by agarose gel electrophoresis, which is not suitable for monitoring individual cells undergoing apoptosis.^[10d,37] A second method is

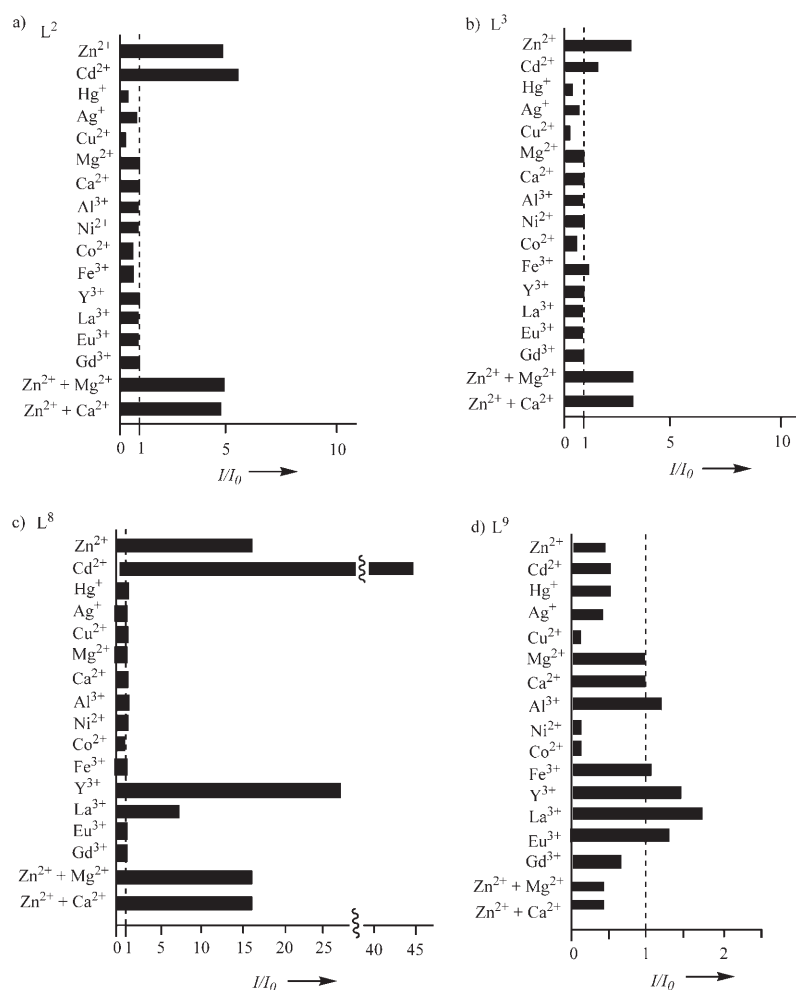


Figure 10. Fluorescent response of **2** (L^2) at 528 nm (a), **4** (L^3) at 416 nm (b), **11** (L^8) at 512 nm (c), and **13** (L^9) at 512 nm (d) to 1 equiv of various metal cations at pH 7.4 [10 mM HEPES with $I=0.1$ (NaNO_3)] at 25 °C ([ligand]=5 μM). I_0 and I are the emission intensities of each ligand at the indicated wavelengths in the absence and presence of metal ions, respectively. The excitation wavelengths were 330 nm for **2**, 368 nm for **4**, and 338 nm for **11** and **13**.

fluorescent labeling with annexin V-dye conjugate^[38] or fluorescent compounds,^[39] which detect phospholipid scrambling on the membranes of apoptotic cells. However, these methods do not reflect intracellular events. Hence, Zn^{2+} fluorophores such as Zinquin^[10] and dansylamidocyclen **2**^[17] have been developed as effective sensors for early-stage apoptosis by detecting free Zn^{2+} in cells.

Figure 13 shows phase-contrast and fluorescence micrographs ($\times 400$) of HeLaS3 cells that were treated with tumor necrosis factor α ($\text{TNF}\alpha$, 1 ng mL^{-1}) and actinomycin D (0.3 $\mu\text{g mL}^{-1}$) for 6 h and then dually stained with propidium iodide (PI)^[19] which stains late-stage apoptotic cells, and **11** (L^8). The typical morphological features of apoptotic cells were observed in Figure 13a (cell shrinkage, decrease in cell volume, and blebbing of membrane). Figure 13b shows fluorescent HeLaS3 cells (actually green) exposed to UV at 330–350 nm to irradiate **11** (L^8), and Figure 13c a fluorescent image (actually red) showing emissions only from PI (excitation at 460–490 nm). We presume that the partially fluores-

cent cells in seen in Figure 13b but not in Figure 13c are early-stage apoptotic cells (indicated by full arrows) and that the fluorescent cells seen in both Figure 13b and c are late-stage apoptotic cells (dashed arrows). We consider that **11** is barely able to discriminate early and late stages of apoptosis. It should also be noted that incubation of HeLaS3 cells with **2** and **11** for 1–3 h did not cause significant damage to cells, although incubation with those ligands for 36 h tends to induce apoptosis.^[19]

Conclusion

We have designed and synthesized a new Zn^{2+} fluorophore, namely 2-(8-hydroxy-5-*N,N*-dimethylaminosulfonylquinolin-yl)methyl cyclen **11** (L^8). UV absorption, fluorescence emission, and ^1H NMR titrations of **11** with Zn^{2+} indicated that **11** forms the 1:1 complex [$\text{Zn}(\text{H}_1\text{L}^8)$] (**12**) with Zn^{2+} , in which N(1) and deprotonated O(8) of the quinolinol moiety coordinate to Zn^{2+} , as proven by single-crystal X-ray diffraction analysis. Interestingly, **11** is almost silent in fluorescent emission in the pH range of 4–8 due to the cyclen moiety. By comparison with the photochemical behaviors of **9c** (L^7) and DPA-based fluorophore **13** (L^9), we conclude that the cyclen moiety has unique properties that quench fluorescence emission of a quinolinol moiety when it is not complexed with metal cations, but enhances emission when complexed with Zn^{2+} or Cd^{2+} . The fluorescent emission of **11** at 512 nm (excitation at 338 nm) increased 17- and 43-fold on complexation with Zn^{2+} and Cd^{2+} , respectively, in aqueous solution at neutral pH. The smaller enhancement in emission by complexation with Zn^{2+} was attributed to the higher Lewis acidity of Zn^{2+} compared to Cd^{2+} . The results of potentiometric pH titrations of **11** with Zn^{2+} strongly suggest that **12** is much more stable than our previous Zn^{2+} fluorophores. The emission of [$\text{Zn}(\text{H}_1\text{L}^8)$] (**12**) at pH 5–10 was almost constant, and this implies that **11** would be useful to determine [Zn^{2+}] over a wide pH range from 5 to 8. We observed a more sensitive response of **11** to Cd^{2+} , whose concentration in cells is very low. Therefore, **11** might offer a

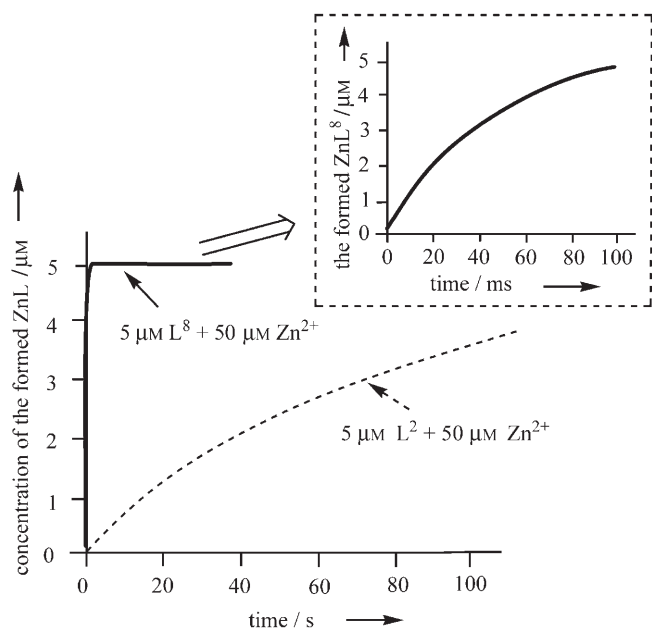
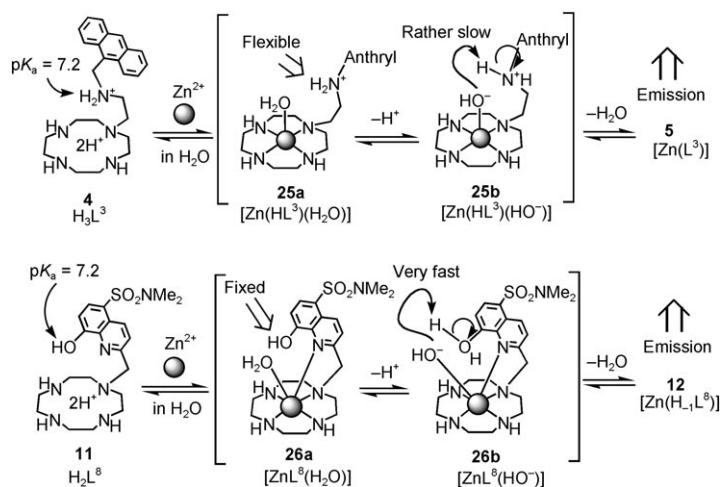


Figure 11. Typical results of time-dependent formation of $[Zn(H_{-1}L^2)]$ (**3**) (dashed curve) and **12** ($Zn(H_{-1}L^8)$) monitored by change in their fluorescence emissions at 510 nm on addition of Zn^{2+} at pH 7.4 [10 mM HEPES with $I=0.1$ ($NaNO_3$)] and $25^\circ C$ (initial $[2 (L^2)]$ and $[11 (L^8)]$ were $5 \mu M$; excitation at 330 nm). The inset shows the results of stopped-flow measurements of $5 \mu M$ **11** under the same conditions.



Scheme 10.

new method of detecting Cd^{2+} in environment samples, industrial waste effluent, and tissue samples.^[40]

We also observed that $[Zn(H_{-1}L^8)]$ (**12**) is both thermodynamically and kinetically stable and that the response of **11** to Zn^{2+} is very quick. Therefore, fast intracellular events involving changes in free $[Zn^{2+}]$ could be detected by utilizing **11**.

A change in the concentration of free Zn^{2+} is reported to be an important factor in the early process of apoptosis. The question whether the changes in free $[Zn^{2+}]$ are a cause or a consequence of apoptosis has yet to be answered.^[10] Un-

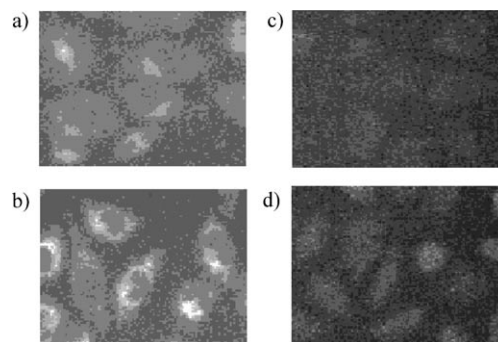


Figure 12. Fluorescent images ($\times 400$) of HeLaS3 cells stained with $50 \mu M$ **2** before (a) and after (b) incubation with $20 \mu M$ Zn^{2+} and $200 \mu M$ pyrithione for 30 min and those stained with $50 \mu M$ **11** before (c) and after (d) incubation with $20 \mu M$ Zn^{2+} and $200 \mu M$ pyrithione for 30 min.

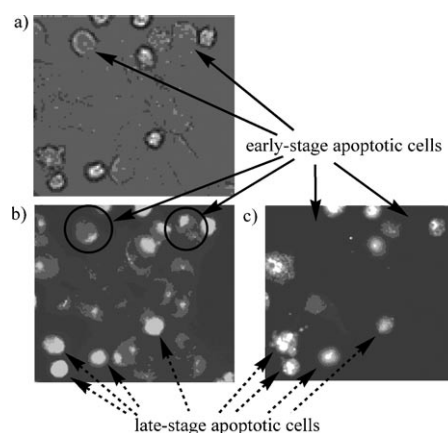


Figure 13. Fluorescent images ($\times 400$) of HeLaS3 cells treated with $TNF\alpha$ ($1 ng mL^{-1}$) and actinomycin D ($0.3 \mu g mL^{-1}$) for 6 h to induce apoptosis and then dually stained with $20 \mu M$ propidium iodide (PI) and $50 \mu M$ **11** (L^8). Phase-contrast image (a), a fluorescent image (by **11**) irradiated with UV light at 330–350 nm showing early- and late-stage apoptotic cells (b), and a fluorescent image (by PI) irradiated with UV light at 460–490 nm showing late-stage apoptotic cells (plain arrows indicate early-stage apoptotic cells and dashed arrows indicate late-stage apoptotic cells) (c).

fortunately, **11** was not as selective for early-stage apoptotic cells over late-stage apoptotic cells as the previous Zn^{2+} fluorophore **2**, possibly due to low cell-membrane permeability and/or the low quantum yield of **11**. Modification of **11** to improve its quantum yield, membrane permeation, and photochemical properties is underway.

Experimental Section

General information: All reagents and solvents were purchased at the highest commercial quality and used without further purification. $Zn(NO_3)_2 \cdot 6H_2O$, $ZnSO_4 \cdot 7H_2O$, $Fe(NO_3)_3 \cdot 9H_2O$, $3CdSO_4 \cdot 8H_2O$, $CuSO_4 \cdot 5H_2O$, and $AgNO_3$ were purchased from Kanto Chemical Co.; $NiSO_4 \cdot 6H_2O$ and $HgCl$ were purchased from Yoneyama Yakuin Kogyo Co.; $Al(NO_3)_3 \cdot 9H_2O$, $CoSO_4 \cdot 7H_2O$, and propidium iodide were purchased from Sigma-Aldrich Chemical Co.; $Y(NO_3)_3 \cdot 6H_2O$, La-

(NO₃)₃·6H₂O, and Eu(NO₃)₃·4H₂O were purchased from Soekawa Co.; and Gd(NO₃)₃·6H₂O was purchased from Wako Pure Chemical Industries, Co. Anhydrous acetonitrile (CH₃CN) was obtained by distillation from calcium hydride or LiAlH₄. All aqueous solutions were prepared using deionized and distilled water. The Good's buffer reagents (Dojindo) were commercially available: MES (2-morpholinoethanesulfonic acid, pK_a=4.8), HEPES (*N*-(2-hydroxyethyl)piperazine-*N'*-2-ethanesulfonic acid, pK_a=7.5), EPPS (3-(4-(2-hydroxyethyl)-1-piperazinyl)propanesulfonic acid, pK_a=8.0), TAPS (*N*-(tris(hydroxymethyl)methylamino)-3-propanesulfonic acid, pK_a=8.4), and CHES (2-(cyclohexylamino)ethanesulfonic acid, pK_a=9.5). Melting points were measured on a Yanaco Melting Point Apparatus and listed without correction. UV spectra were recorded on a Hitachi U-3500 spectrophotometer and JASCO UV/VIS spectrophotometer V-550, and fluorescence (excitation and emission) spectra were recorded on a Hitachi F-4500 fluorescence spectrophotometer and JASCO FP-6500 spectrofluorometer at 25 ± 0.1 °C. The data from UV titrations (increases or decreases in ε values at a given wavelength) and fluorescence titrations (increases or decreases in fluorescence emission intensity at a given wavelength) were analyzed for apparent complexation constants K_{app} by using the program Bind Works (Calorimetry Sciences Corp). The fluorescence quantum yield Φ was determined by comparison with the integrated corrected emission spectrum of a quinine sulfate standard, whose quantum yield in 0.1 M H₂SO₄ was assumed to be 0.55 (excitation at 366 nm). IR spectra were recorded on a Horiba FTIR-710 spectrophotometer at room temperature. ¹H (400 MHz) and ¹³C (100 MHz) NMR spectra at 35 ± 0.1 °C were recorded on a JEOL Lambda 400 spectrometer. ¹H (300 MHz) and ¹³C (75 MHz) NMR spectra were recorded on a JEOL Always 300 spectrometer. Tetramethylsilane was used as an internal reference for ¹H and ¹³C NMR measurements in CDCl₃ and CD₃CN. [2,2,3,3-D₄]-3-(Trimethylsilyl)propionic acid sodium salt (TSP) was used as external reference for ¹H and ¹³C NMR measurements in D₂O. The pD values in D₂O were corrected for deuterium isotope effect by using pD = (pH-meter reading) + 0.40. Elemental analyses were performed on a Perkin-Elmer CHN 2400 analyzer. TLC and silica-gel column chromatographies were performed using a Merck 5554 (silica gel) TLC plates and Fuji Silysia Chemical FL-100D, respectively.

8-Benzenesulfonyloxy-2-bromomethyl-5-*N,N*-dimethylaminosulfonylquinoline (19): Benzenesulfonyl chloride (1.3 g, 7.1 mmol) was added dropwise to a solution of 8-hydroxy-2-methyl-5-*N,N*-dimethylaminosulfonylquinoline^[24] (780 mg, 6.4 mmol) and Et₃N (780 mg, 7.7 mmol) in CHCl₃ (13 mL) at 0 °C over 1 h. After the reaction mixture had been stirred for 1.5 h at room temperature, H₂O (5 mL) was added and stirring was continued for 0.5 h. The reaction mixture was extracted from saturated K₂CO₃ with CH₂Cl₂, and the organic layer was dried with anhydrous K₂CO₃, filtered, and concentrated under reduced pressure. The residue was purified by silica-gel column chromatography (hexane/AcOEt) to give 8-benzenesulfonyloxy-2-methyl-5-*N,N*-dimethylaminosulfonylquinoline (2.5 g, 96 % yield) as a colorless amorphous solid. A mixture of 8-benzenesulfonyloxy-2-methyl-5-*N,N*-dimethylaminosulfonylquinoline (1.5 g, 3.7 mmol), *N*-bromosuccinimide (380 mg, 2.6 mmol), and AIBN (40 mg, 0.24 mmol) in distilled CCl₄ (190 mL) was stirred at reflux under an argon atmosphere for 8 h (*N*-bromosuccinimide was added portionwise), and the reaction mixture was concentrated under reduced pressure. The residue was dissolved in CH₂Cl₂ and washed with a mixture of Na₂CO₃ and Na₂S₂O₄ in aqueous solution. The residue was purified by silica-gel column chromatography (hexane/AcOEt) to afford **19** as a colorless amorphous solid (250 mg, 14 % yield). The starting material (8-benzenesulfonyloxy-2-methyl-5-*N,N*-dimethylaminosulfonylquinoline) was recovered in 56 % yield (860 mg). ¹H NMR (400 MHz, CDCl₃/TMS): δ = 2.83 (s, 6H), 4.42 (s, 2H), 7.52 (t, *J*₃ = 7.8 Hz, 2H; ArH), 7.65 (d, *J* = 7.4 Hz, 1H; ArH), 7.67 (d, *J* = 8.9 Hz, 1H; ArH), 7.80 (d, *J* = 8.3 Hz, 1H ArH), 8.00 (d, *J* = 8.5 Hz, 2H; ArH), 8.18 (d, *J* = 8.3 Hz, 1H; ArH), 9.05 ppm (d, *J* = 9.0 Hz, 2H; ArH); ¹³C NMR (100 MHz, CDCl₃/TMS): δ = 33.08, 37.42, 121.9, 123.4, 125.4, 129.0, 130.2, 132.0, 134.4, 135.9, 140.9, 149.0, 158.1 ppm; IR (KBr): $\tilde{\nu}$ = 3092, 2921, 1706, 1596, 1498, 1460, 1375, 1343, 1189, 1147, 1054, 957, 799, 619 cm⁻¹.

1-(8-Benzenesulfonyloxy-5-*N,N*-dimethylaminosulfonylquinolin-2-ylmethyl)-4,7,10-tris(*tert*-butyloxycarbonyl)-1,4,7,10-tetraazacyclododecane (20):

A mixture of **18** (0.59 g, 1.2 mmol),^[26] **19** (0.66 g, 1.4 mmol), and Na₂CO₃ (0.2 g, 2.1 mmol) in CH₃CN (50 mL) was stirred at 60 °C under an argon atmosphere overnight. After insoluble inorganic salts were filtered off, the filtrate was concentrated under reduced pressure. The residue was purified by silica-gel column chromatography (hexane/AcOEt) to afford **20** as a pale-yellow amorphous solid (1.0 g, 92 % yield). ¹H NMR (400 MHz, CDCl₃/TMS): δ = 1.42–1.54 (br, 27H), 2.83 (s, 6H), 2.78–3.56 (br, 16H), 3.96 (s, 2H), 7.53 (dd, *J* = 8.0, 8.0 Hz, 2H; ArH), 7.61 (d, *J* = 8.3 Hz, 2H; ArH), 7.65 (dd, *J* = 4.4 Hz, 1H; ArH), 8.00 (dd, *J* = 7.1, 1.2 Hz, 2H; ArH), 8.11 (d, *J* = 8.0 Hz, 1H; ArH), 8.96 ppm (d, *J* = 8.9 Hz, 1H; ArH); ¹³C NMR (100 MHz, CDCl₃/TMS): δ = 28.46, 28.69, 36.62, 37.38, 47.78, 49.89, 54.21, 55.14, 57.05, 79.50, 81.30, 120.4, 124.4, 128.3, 128.5, 129.1, 129.5, 131.7, 133.5, 134.3, 136.3, 141.3, 149.1 ppm; IR (KBr): $\tilde{\nu}$ = 2975, 2931, 1685, 1415, 1365, 1250, 1154, 1059, 976, 956, 808, 727, 599 cm⁻¹.

1-(8-Hydroxy-5-*N,N*-dimethylaminosulfonylquinolin-2-ylmethyl)-1,4,7,10-tetraazacyclododecane (21): A 28 % aqueous NH₃ solution (35 mL) was added to a solution of **20** (1.0 g, 1.1 mmol) in MeOH (40 mL), and the mixture was stirred at reflux for 5 d. The reaction mixture was concentrated under reduced pressure, and the residue was purified by silica-gel column chromatography (CH₂Cl₂/MeOH) to afford **21** as a pale yellow amorphous solid (0.82 g, 97 % yield): ¹H NMR (400 MHz, CD₃OD/TMS): δ = 0.91–1.49 (m, 27H), 2.68–2.77 (br, 10H), 3.30 (s, 6H), 3.31–3.64 (br, 10H), 4.12 (s, 2H), 7.20 (d, *J* = 8.3 Hz, 1H; ArH), 7.75 (d, *J* = 8.5 Hz, 1H; ArH), 8.10 (d, *J* = 8.5 Hz, 1H; ArH), 9.01 ppm (d, *J* = 9.0 Hz, 1H; ArH); ¹³C NMR (100 MHz, CD₃OD/TMS): δ = 28.9, 29.1, 37.8, 56.0, 56.1, 57.4, 57.5, 57.7, 59.1, 81.2, 81.3, 95.5, 95.6, 97.3, 110.2, 115.4, 120.7, 123.0, 125.8, 126.2, 134.0, 135.4, 139.2, 140.9, 157.4, 157.5, 157.9, 159.2, 159.6 ppm; IR (KBr): $\tilde{\nu}$ = 2974, 1689, 1564, 1502, 1462, 1415, 1365, 1320, 1251, 1154, 959, 858, 773, 716, 548 cm⁻¹.

1-(8-Hydroxy-5-*N,N*-dimethylaminosulfonylquinolin-2-ylmethyl)-1,4,7,10-tetraazacyclododecane tetrahydrochloride salt (11·4HCl·2H₂O·0.2EtOH): Aqueous HCl (1 M, 10 mL) was added dropwise to a solution of **21** (0.5 g, 0.68 mmol) in MeOH (30 mL) at 0 °C, and the mixture was stirred overnight at room temperature. The reaction mixture was concentrated under reduced pressure, and the remaining solids were recrystallized from EtOH/H₂O to give 11·4HCl·2H₂O·0.2EtOH as pale yellow needles (0.39 g, 89 % yield). M.p. 196–197 °C; ¹H NMR (400 MHz, D₂O/TSP): δ = 2.81 (s, 6H), 3.08–3.37 (m, 16H), 4.24 (s, 2H), 7.34 (d, *J* = 3.3 Hz, 1H; ArH), 7.66 (d, *J* = 9.0 Hz, 1H; ArH), 8.17 (d, *J* = 8.6 Hz, 1H; ArH), 9.00 ppm (d, *J* = 9.0 Hz, 1H; ArH); ¹³C NMR (100 MHz, D₂O): δ = 39.6, 44.9, 45.3, 52.3, 60.4, 98.7, 113.7, 123.7, 126.3, 128.3, 135.7, 137.8, 141.0, 159.8, 161.2 ppm; IR (KBr): $\tilde{\nu}$ = 3433, 2963, 1643, 1560, 1456, 1383, 1330, 1156, 951, 721, 474 cm⁻¹; elemental analysis calcd (%) for C_{20.4}H_{43.2}Cl₄N₆O_{6.2}S (645.67): C 37.95, H 6.74, N 13.02, S 4.97; found: C 37.50, H 7.23, N 13.21, S 5.39.

For X-ray crystal structure analysis, 11·4HCl·3H₂O·0.2EtOH (H₄L⁸) (50 mg, 0.077 mmol) was recrystallized from aqueous solution at pH 10 (adjusted with NaOH) to give **11** in the H₂(H₋₁)L⁸ form (26 mg, 62 % yield). M.p. >250 °C; ¹H NMR (400 MHz, D₂O/TSP): δ = 2.81 (s, 6H), 3.08–3.37 (m, 16H), 4.24 (s, 2H), 6.85 (d, *J* = 8.8 Hz, 1H), 7.45 (d, *J* = 8.8 Hz, 1H; ArH), 8.02 (d, *J* = 8.8 Hz, 1H; ArH), 8.86 ppm (d, *J* = 9.1 Hz, 1H; ArH); elemental analysis calcd (%) for C₂₀H₄₁ClN₆O₇S (545.09): C 44.07; H 7.58; N 15.42; S 5.88; found: C 44.35; H 7.90; N 15.26; S 5.60.

1-(8-Hydroxy-5-*N,N*-dimethylaminosulfonylquinolin-2-ylmethyl)-1,4,7,10-tetraazacyclododecane Zn(ClO₄) complex (12·ClO₄; [Zn(H₋₁L⁸)]ClO₄): An aqueous solution of Zn(ClO₄)₂·6H₂O (27 mg, 0.072 mmol) in H₂O (3 mL) was added to a solution of 11·4HCl·3H₂O·0.2EtOH (40 mg, 0.062 mmol) in H₂O (10 mL) at room temperature, and the pH of the reaction mixture was adjusted to 7.5 with 0.1 M NaOH. After the insoluble compounds were filtered off, the filtrate was slowly concentrated under reduced pressure to obtain 12·ClO₄ ([Zn(H₋₁L⁸)]ClO₄) as pale yellow prisms (15 mg, 40 % yield). M.p. >250 °C; ¹H NMR (400 MHz, D₂O/TSP): δ = 2.73 (s, 6H), 2.78–3.25 (m, 16H), 4.32 (s, 2H), 6.96 (d, *J* = 8.8 Hz, 1H), 7.65 (d, *J* = 8.8 Hz, 1H; ArH), 8.09 (d, *J* = 8.8 Hz, 1H; ArH), 9.00 ppm (d, *J* = 9.2 Hz, 1H; ArH); ¹³C NMR (D₂O): δ = 36.41, 43.34, 44.29, 44.57, 52.90, 57.77, 110.6, 121.6, 125.0, 134.9, 136.3, 137.9, 154.8, 165.1 ppm; IR (KBr): 3279, 2915, 2870, 1563, 1469, 1678, 1101, 949,

835, 718, 539 cm⁻¹; elemental analysis calcd (%) for C₂₀H₃₁ClN₆O₇SZn (600.39): C 40.01, H 5.20, N 14.00, S 5.34; found: C 39.92, H 5.19, N 13.89, S 5.48.

Crystallographic study of 11 (H₂(H₋₁L⁸)Cl): C₂₀H₄₁ClN₆O₇S, M_r = 545.09, pale yellow prismatic, crystal size 0.35 × 0.20 × 0.10 mm, monoclinic, space group P2₁/c (No. 14), a = 18.029(20), b = 10.785(11), c = 13.913(16) Å, β = 90.47(5)°, V = 2705(5) Å³, Z = 4, ρ_{calcd} = 1.338 g cm⁻³, 31462 measured reflections, 7808 unique reflections (R_{int} = 0.059), 2θ_{max} = 59.9°, R1 = 0.0448 [calculated for 3439 reflections with I > 2σ(I)], R_w = 0.0949 (for all reflections), GOF = 0.982.

Crystallographic study of 12-ClO₄ ([Zn(H₋₁L⁸)]ClO₄): C₂₀H₃₁ClN₆O₇SZn, M_r = 600.39, pale yellow prisms, crystal size 0.20 × 0.07 × 0.03 mm, orthorhombic, space group Aea2 (No. 41), a = 30.575(17), b = 12.504(7), c = 13.028(8) Å, V = 4981(5) Å³, Z = 8, ρ_{calcd} = 1.601 g cm⁻³, 20932 measured reflections, 5602 unique reflections (R_{int} = 0.162), 2θ_{max} = 55.0°, R1 = 0.0752 [calculated for 2695 reflections with I > 2σ(I)], R_w = 0.1413 (for all reflections), GOF = 0.929.

All measurements were made on a Rigaku RAXIS-RAPID imaging plate area detector with graphite-monochromated MoK_α radiation at 93 K. The structures were solved by direct methods and refined by full-matrix least-squares techniques. All calculations were performed using CrystalStructure crystallographic software package, except for solving phase problems and refinements, which were done with SHELXS97 and SHELXL97, respectively.

CCDC 601452 (**11**, HL⁸), 601453 (**12**, [Zn(H₋₁L⁸)]), and 641454 (**30**, Cu(H₋₁L⁸)) contain the supplementary crystallographic data for this paper. These data can be obtained free of charge from the Cambridge Crystallographic Data Centre via www.ccdc.cam.ac.uk/data_request/cif.

Potentiometric pH titrations: The preparation of the test solutions and the calibration method of the electrode system (Potentiometric Automatic Titrator AT-400 and Auto Piston Buret APB-410, Kyoto Electronics Manufacturing, Co. Ltd.) with Orion Research Ross Combination pH Electrode 8102BN) were described earlier.^[17,19–21] All the test solutions (50 mL) were kept under an argon (> 99.999% purity) atmosphere. The potentiometric pH titrations were performed with I = 0.10 (NaNO₃) at 25.0 ± 0.1 °C, and at least two independent titrations were performed (0.1 M aqueous NaOH was used as base). Deprotonation constants of Zn²⁺-bound water K₂' (= [HO⁻-bound species][H⁺]/[H₂O-bound species]) were determined by means of the program BEST.^[25] All the sigma fit values defined in the program are smaller than 0.05. The K_w (= a_{H+}a_{OH-}), K_w' (= [H⁺][OH⁻]), and f_{H+} values used at 25 °C were 10^{-14.00}, 10^{-13.79}, and 0.825, respectively. The corresponding mixed constants K₂ (= [HO⁻-bound species]a_{H+}/[H₂O-bound species]), were derived by using [H⁺] = a_{H+}/f_{H+}. The percentage species distribution values against pH (= -log [H⁺] + 0.084) were obtained using the program SPE.^[25]

Kinetic and stopped-flow measurements on Zn²⁺ complexation of 2, 4, 11, and 13: Kinetic measurements on the Zn²⁺ complexation of **2** (L²) and **4** (L³) (initial [2] = [4] = 10 μM) were done in 10 mM HEPES [pH 7.4 with I = 0.1 (NaNO₃)] at 25 ± 0.1 °C by monitoring fluorescence emission on a JASCO FP-6500 spectrofluorometer. For very fast Zn²⁺ complexation of **11** and **13**, stopped-flow measurements were carried out in 10 mM HEPES [pH 7.4 with I = 0.1 (NaNO₃)] at 25 ± 0.1 °C by monitoring emission of **11** (L⁸) and **13** (L⁹) at 500 nm with a stopped-flow light-scattering spectrophotometer (model SX. 18MV, Applied Photophysics Ltd., Surrey, UK).

Treatment of HeLaS3 cells with Zn²⁺ ionophore and fluorescence microscopy:^[19] HeLaS3 cells were maintained in Dulbecco's Modified Eagle Medium (DMEM) (Sigma) supplemented with 10% FBS (Sanko Junyaku, Japan), 100 μg mL⁻¹ streptomycin, and 100 units mL⁻¹ penicillin. HeLaS3 cells were seeded into 35 mm glass-bottomed dishes. The cells were treated with 20 μM ZnSO₄·7H₂O and 200 μM pyrithione in culture medium for 30 min in a humidified atmosphere of 5% CO₂ at 37 °C. The cells were then washed three times with PBS to remove extracellular Zn²⁺ and incubated with Zn²⁺ fluorophores **2** and **11**. The cells were observed by phase contrast and UV fluorescence microscopy (Olympus fluorescence microscope; excitation at 330–385 nm, emission at 500 nm for **11**, and excitation at 460–490 nm, emission at 590 nm for PI).

Observing apoptotic morphology in HeLaS3 cells and detecting apoptosis with 11: HeLaS3 cells were seeded into 35 mm cell culture dishes each containing a cover slip. The dishes were incubated under a humidified atmosphere of 5% CO₂ at 37 °C. The cells were treated with TNFα (1 ng mL⁻¹) and actinomycin D (0.3 μg mL⁻¹) for 6 h. The culture medium was replaced with 1 mL of fresh culture medium containing 50 μM **11** and 30 μM propidium iodide (PI). The reaction mixture was incubated at 37 °C under a humidified atmosphere of 5% CO₂ for 30 min and rinsed once with 1 mL of PBS for fluorescent microscopy.

Acknowledgements

S.A. is grateful for a Grant-in-Aid from the Ministry of Education, Science and Culture in Japan (No. 15590008) and for grants from the Mitsubishi Chemical Corporation Fund (Tokyo), Toray Science Foundation (Tokyo), Terumo Life Science Foundation (Kanagawa), Mochida Memorial Foundation for Medical and Pharmaceutical Research (Tokyo), and The Novartis Foundation (Japan). We thank Mr. Shinya Kondo, Mrs. Chika Tsuji, and Mr. Yoji Uno (Tega Science Inc., Japan) for stopped-flow experiments. We thank NMR instruments (for the use of a JEOL Alpha (400 MHz)) in the Research Center for Molecular Medicine (RCMM) at Hiroshima University.

- a) J. J. R. Fraústo da Silva, R. J. P. Williams, *The Biological Chemistry of the Elements*, Clarendon, Oxford, **1991**; b) R. J. P. Williams, J. J. R. Fraústo da Silva, *Coord. Chem. Rev.* **2000**, 200–202, 247–348.
- a) B. L. Valee, K. H. Falchuk, *Physiol. Rev.* **1993**, 73, 91–118; b) W. N. Lipscomb, N. Sträter, *Chem. Rev.* **1996**, 96, 2375–2433; c) D. A. Auld in *Handbook of Metalloprotein* (Eds.: I. Bertini, A. Sigel, H. Sigel), Marcel Dekker, New York, **2001**, pp. 881–959; d) D. S. Auld, *BioMetals* **2001**, 14, 271–313; e) S. Aoki, E. Kimura in *Comprehensive Coordination Chemistry II*, Vol. 8 (Eds.: L. Que, Jr., W. B. Tolman), Elsevier, Amsterdam, **2004**, pp. 601–640; f) W. Maret, *J. Trace Elem. Med. Biol.* **2005**, 19, 7–12.
- a) N. P. Pavletich, C. O. Pabo, *Science* **1993**, 261, 1701–1707; b) J. M. Berg, Y. Shi, *Science* **1996**, 271, 1081–1085; c) M. Papworth, P. Kolasinska, M. Minczuk, *Gene* **2005**, 366, 27–38.
- a) C. J. Frederickson, E. J. Kasarski, D. Ringo, R. E. Frederickson, *J. Neurosci. Methods* **1987**, 20, 91–103; b) C. J. Frederickson, *Int. Rev. Neurobiol.* **1989**, 145, 145–238; c) M. P. Cuajungco, G. J. Lees, *Neurobiol. Dis.* **1997**, 4, 137–169; d) D. W. Choi, J. Y. Koh, *Annu. Rev. Neurosci.* **1998**, 21, 347–375; e) C. J. Frederickson, A. I. Bush, *BioMetals* **2001**, 14, 353–366; f) A. Takeda, *BioMetals* **2001**, 14, 343–351; g) S. C. Burdette, S. J. Lippard, *Coord. Chem. Rev.* **2001**, 216–217, 333–361; h) S. C. Burdette, S. J. Lippard, *Proc. Natl. Acad. Sci. USA* **2003**, 100, 3605–3610.
- a) A. J. Schetz, D. R. Sibley, *J. Neurochem.* **1997**, 68, 1990–1997; b) G. Swaminath, T. W. Lee, B. Kobilka, *J. Biol. Chem.* **2003**, 278, 352–356; c) Y. Liu, M. M. Teeter, C. J. DuRand, K. A. Neve, *Biochem. Biophys. Res. Commun.* **2006**, 339, 873–879.
- a) S. Treves, P. L. Trentini, M. Ascannelli, G. Buccì, F. di Virgilio, *Exp. Cell Res.* **1994**, 211, 339–343; b) D. K. Perry, M. J. Smyth, H. R. Stennicke, G. S. Salvesen, P. Duriez, G. G. Poirier, Y. A. Hannun, *J. Biol. Chem.* **1997**, 272, 18530–18533; c) A. O. Truong-Tran, J. Carter, R. E. Ruffin, P. D. Zalewski, *BioMetals* **2001**, 14, 315–330.
- a) R. D. Palmiter, S. D. Findley, *EMBO J.* **1995**, 14, 69–649; b) S. L. Sensi, L. M. T. Canzoniero, S. P. Yu, H. S. Ying, J.-Y. Koh, G. A. Kerchner, D. W. Choi, *J. Neurosci.* **1997**, 17, 9554–9564; c) C. E. Outten, T. V. O'Halloran, *Science* **2001**, 292, 2488–2492; d) L. A. Finney, T. V. O'Halloran, *Science* **2003**, 300, 931–936; e) K. H. Thompson, C. Orvig, *Science* **2003**, 300, 936–936.
- a) R. P. Haugland, *Handbook of Fluorescent Probes and Research Products*, 9th ed., Molecular Probes, Eugene, OR, **2002**; b) B. Valeur, *Molecular Fluorescence: Principles and Applications*, Wiley, New York, **2002**; c) A. Prasanna de Silva, H. Q. Nimal Gunaratne, T. Gunnlaugsson, A. J. M. Huxley, C. P. McCoy, J. T. Rademacher,

- T. E. Rice, *Chem. Rev.* **1997**, *97*, 1515–1566; d) B. Valeur, I. Leray, *Coord. Chem. Rev.* **2000**, *205*, 3–40; e) L. Prodi, F. Bolletta, M. Montalti, N. Zaccheroni, *Coord. Chem. Rev.* **2000**, *205*, 59–83; f) E. Kimura, S. Aoki, *BioMetals* **2001**, *14*, 191–204; g) P. Jiang, Z. Guo, *Coord. Chem. Rev.* **2004**, *248*, 205–209; h) K. Kikuchi, K. Komatsu, T. Nagano, *Curr. Opin. Chem. Biol.* **2004**, *8*, 182–191; i) N. C. Lim, H. C. Freaake, C. Brückner, *Chem. Eur. J.* **2005**, *11*, 38–49.
- [9] a) P. D. Zalewski, S. H. Millard, I. J. Forbes, O. Kapaniris, A. Slavotinek, W. H. Betts, A. D. Ward, S. F. Lincoln, I. Mahadevan, *J. Histochem. Cytochem.* **1994**, *42*, 877–884; b) K. M. Hendrickson, T. Rodopoulos, P.-A. Pittet, I. Mahadevan, S. F. Lincoln, A. D. Ward, T. Kurucsev, P. A. Duckworth, I. J. Forbes, P. D. Zalewski, H. Betts, *J. Chem. Soc. Dalton Trans.* **1997**, 3879–3882; c) D. Berendji, V. Kolb-Bachofen, K. L. Meyer, O. Grapenthin, H. Weber, V. Wahn, K.-D. Kröncke, *FEBS Lett.* **1997**, *405*, 37–41; d) C. J. Fahrni, T. V. O'Halloran, *J. Am. Chem. Soc.* **1999**, *121*, 11448–11458; e) M. S. Nasir, C. J. Fahrni, D. A. Suhy, K. J. Kolodisick, C. P. Singer, T. V. O'Halloran, *J. Biol. Inorg. Chem.* **1999**, *4*, 775–783; f) K. M. Hendrickson, J. P. Geue, O. Wyness, S. F. Lincoln, A. D. Ward, *J. Am. Chem. Soc.* **2003**, *125*, 3889–3895.
- [10] a) P. D. Zalewski, I. J. Forbes, C. Giannakis, *Biochem. Int.* **1991**, *24*, 1093–1101; b) P. D. Zalewski, I. J. Forbes, W. H. Betts, *Biochem. J.* **1993**, *296*, 403–408; c) P. Coyle, P. D. Zalewski, J. C. Philcox, I. J. Forbes, A. D. Ward, S. F. Lincoln, I. Mahadevan, A. M. Rofe, *Biochem. J.* **1994**, *303*, 781–786; d) P. D. Zalewski, I. J. Forbes, R. F. Seamark, R. Borlinghaus, W. H. Betts, S. F. Lincoln, A. D. Ward, *Chem. Biol.* **1994**, *1*, 153–161.
- [11] a) G. K. Walkup, S. C. Burdette, S. J. Lippard, R. Y. Tsien, *J. Am. Chem. Soc.* **2000**, *122*, 5644–5645; b) S. C. Burdette, G. K. Walkup, B. Spingler, R. Y. Tsien, S. J. Lippard, *J. Am. Chem. Soc.* **2001**, *123*, 7831–7841; c) S. C. Burdette, C. J. Frederickson, W. Bu, S. J. Lippard, *J. Am. Chem. Soc.* **2003**, *125*, 1778–1787; d) C. C. Woodrooffe, S. J. Lippard, *J. Am. Chem. Soc.* **2003**, *125*, 11458–11459.
- [12] a) T. Hirano, K. Kikuchi, Y. Urano, T. Higuchi, T. Nagano, *Angew. Chem. Int. Ed.* **2000**, *39*, 1052–1055; b) T. Hirano, K. Kikuchi, Y. Urano, T. Higuchi, T. Nagano, *J. Am. Chem. Soc.* **2000**, *122*, 12399–12400; c) T. Hirano, K. Kikuchi, Y. Urano, T. Nagano, *J. Am. Chem. Soc.* **2002**, *124*, 6555–6562; d) K. Maruyama, K. Kikuchi, T. Hirano, Y. Urano, T. Nagano, *J. Am. Chem. Soc.* **2002**, *124*, 10650–10651; e) K. Hanaoka, K. Kikuchi, H. Kojima, Y. Urano, T. Nagano, *Angew. Chem.* **2003**, *115*, 3104–3107; *Angew. Chem. Int. Ed.* **2003**, *42*, 2996–2999.
- [13] a) Z. Dai, X. Xu, J. W. Canary, *Chem. Commun.* **2002**, 1414–1415; b) M. Royzen, A. Durandini, V. G. Young, Jr., N. E. Geacintov, J. W. Canary, *J. Am. Chem. Soc.* **2006**, *128*, 3851–3852; c) T. Taki, J. L. Wolford, T. V. O'Halloran, *J. Am. Chem. Soc.* **2004**, *126*, 712–713; d) N. C. Lim, C. Brückner, *Chem. Commun.* **2004**, 1094–1095.
- [14] a) O. Reany, T. Gunnlaugsson, D. Parker, *Chem. Commun.* **2000**, 473–474; b) J. S. Marvin, H. W. Hellinga, *Proc. Natl. Acad. Sci. USA* **2001**, *98*, 4955–4960; c) C. A. Fierke, R. B. Thompson, *BioMetals* **2001**, *14*, 205–222; d) R. T. Bronson, J. S. Bradshaw, P. B. Savage, S. Fuangwasdi, S. C. Lee, K. E. Krakowiak, R. M. Izatt, *J. Org. Chem.* **2001**, *66*, 4752–4758; e) R. T. Bronson, J. S. Bradshaw, P. B. Savage, S. Fuangwasdi, S. C. Lee, K. E. Krakowiak, R. M. Izatt, *J. Org. Chem.* **2001**, *66*, 4752–4758; f) P. Jiang, L. Chen, J. Lin, Q. Liu, J. Ding, X. Gao, Z. Guo, *Chem. Commun.* **2002**, 1424–1425; g) K. R. Gee, Z.-J. Zhou, W.-J. Qian, R. Kennedy, *J. Am. Chem. Soc.* **2002**, *124*, 776–777; h) S. L. Sensi, D. Ton-That, J. H. Weiss, A. Roth, K. R. Gee, *Cell Calcium* **2003**, *34*, 281–284; i) M. S. Han, D. H. Kim, *Supramol. Chem.* **2003**, *15*, 59–64; j) M. M. Henary, Y. Wu, C. J. Fahrni, *Chem. Eur. J.* **2004**, *10*, 3015–3025.
- [15] a) E. Kimura, T. Koike, M. Shionoya, *Struct. Bonding* **1997**, *89*, 1–28; b) E. Kimura, T. Koike in *Compr. Supramol. Chem.* **1996**, *10*, 429–444; c) E. Kimura, T. Koike, *Chem. Commun.* **1998**, 1495–1500; d) E. Kimura, T. Koike, in *Bioinorganic Catalysis* (Eds.: J. Reedijk, E. Bouwman), Marcel Dekker, New York, **1999**, pp. 33–54; e) E. Kimura, E. Kikuta, *J. Biol. Inorg. Chem.* **2000**, *5*, 139–155; f) E. Kimura, *Curr. Opin. Chem. Biol.* **2000**, *4*, 207–213; g) E. Kimura, *Acc. Chem. Res.* **2001**, *34*, 171–179; h) S. Aoki, E. Kimura, *Rev. Mol. Biotechnol.* **2002**, *90*, 129–155; i) S. Aoki, E. Kimura, *Chem. Rev.* **2004**, *104*, 769–788.
- [16] A. E. Martell, R. D. Hancock, *Metal Complexes in Aqueous Solutions*, Plenum, New York, **1996**.
- [17] a) T. Koike, T. Watanabe, S. Aoki, E. Kimura, M. Shiro, *J. Am. Chem. Soc.* **1996**, *118*, 12696–12703; b) E. Kimura, *S. Afr. J. Chem.* **1997**, *50*, 240–248; c) E. Kimura, T. Koike, *Chem. Soc. Rev.* **1998**, *27*, 179–184.
- [18] G. Xie, J. S. Bradshaw, H. Song, T. Bronson, P. B. Savage, K. E. Krakowiak, R. M. Izatt, L. Prodi, M. Montalti, N. Zaccheroni, *Tetrahedron* **2001**, *57*, 87–91.
- [19] a) E. Kimura, S. Aoki, E. Kikuta, T. Koike, *Proc. Natl. Acad. Sci. USA* **2003**, *100*, 3731–3736; b) E. Kimura, R. Takasawa, S. Tanuma, S. Aoki, *Science STKE* **2004**, 223, pl7.
- [20] S. Aoki, S. Kaido, H. Fujioka, E. Kimura, *Inorg. Chem.* **2003**, *42*, 1023–1030.
- [21] S. Aoki, D. Kagata, M. Shiro, K. Takeda, E. Kimura, E. *J. Am. Chem. Soc.* **2004**, *126*, 13377–13390.
- [22] W. R. Steitz, *Crit. Rev. Anal. Chem.* **1980**, *8*, 367–405.
- [23] G. K. Walkup, B. Imperiali, *J. Org. Chem.* **1998**, *63*, 6727–6731.
- [24] D. A. Pearce, N. Jotterand, I. S. Carrico, B. Imperiali, *J. Am. Chem. Soc.* **2001**, *123*, 5160–5161.
- [25] A. E. Martell, R. J. Motekaitis, *Determination and Use of Stability Constants*, 2nd ed., VCH, New York, **1992**.
- [26] E. Kimura, S. Aoki, T. Koike, M. Shiro, *J. Am. Chem. Soc.* **1997**, *119*, 3068–3076.
- [27] For the synthesis of **13** (L^9), see Supporting Information.
- [28] a) E. Kimura, T. Shiota, T. Koike, M. Shiro, M. Kodama, M. *J. Am. Chem. Soc.* **1990**, *112*, 5805–5811; b) E. Kimura, M. Shionoya, A. Hoshino, T. Ikeda, Y. Yamada, *J. Am. Chem. Soc.* **1992**, *114*, 10134–10137; c) M. Shionoya, E. Kimura, M. Shiro, *J. Am. Chem. Soc.* **1993**, *115*, 6730–6737.
- [29] We do not exclude the possibility that complex behavior of **13** is due to its aggregation in aqueous solution, as suggested by one of the referees.
- [30] S. Aoki, H. Kawatani, T. Goto, E. Kimura, M. Shiro, *J. Am. Chem. Soc.* **2001**, *123*, 1123–1132.
- [31] For a discussion of excited-state processes in 8-quinolinol, see E. Bardez, I. Devol, B. Larrey, B. Valeur, *J. Phys. Chem. B* **1997**, *101*, 7786–7793.
- [32] The dissociation constant of the 1:1 complex $[Zn(H_1L^9)]$ was estimated to be <50 nM at pH 7.4 and 25 °C with $I=0.1$ (NaNO₃).
- [33] Note that the Cu–N(1) bond length (2.34 Å) is somewhat longer than other Cu–N(cyclen) bond lengths (2.10, 2.01, and 2.09 Å) and the Cu–N(quinoline) bond length (2.00 Å).
- [34] By potentiometric pH titrations, the intrinsic $\log K_s([Cd(H_1L^8)])$ was determined to be 21.5 ± 0.1 , and the apparent $\log K_{app}([Cd(H_1L^8)])$ at pH 7.4 was calculated to be 13.6 ± 0.1 . The intrinsic $\log K_s([Cu(H_1L^8)])$ was too large to be determined by potentiometric pH titrations.
- [35] For emission intensities of **12** ($[Zn(H_1L^8)]$, 5 μ M) at 512 nm in the pH range of 4.5–11, see Supporting Information.
- [36] a) B. Beutler, C. van Huffel, *Science* **1994**, *264*, 667–668; b) G. Evans, T. Littlewood, *Science* **1998**, *281*, 1317–1322.
- [37] a) C. Giannakis, I. J. Forbes, P. D. Zalewski, *Biochem. Biophys. Res. Commun.* **1991**, *181*, 915–920; b) I. J. Forbes, P. D. Zalewski, C. Giannakis, P. A. Cowled, *Exp. Cell Res.* **1992**, *198*, 367–372; c) D. Shiokawa, H. Ohyama, T. Yamada, S. Tanuma, *Biochem. J.* **1997**, *326*, 675–681; d) H. Yao, R. Takasawa, K. Fukuda, D. Shiokawa, F. Sadanaga-Akiyoshi, S. Ibayashi, S. Tanuma, H. Uchimura, *Mol. Brain Res.* **2001**, *91*, 112–118.
- [38] I. Vermes, C. Haanen, H. Stefferns-Nakken, C. Reutelingsperger, *J. Immunol. Methods* **1995**, *184*, 39–51.
- [39] a) C. Lakshmi, R. G. Hanshaw, B. D. Smith, *Tetrahedron* **2004**, *60*, 11307–11315; b) R. G. Hanshaw, C. Lakshmi, T. N. Lambert, J. R. Johnson, B. D. Smith, *ChemBioChem* **2005**, *6*, 2214–2220; c) A. Zweifach, *Biochem. J.* **2000**, *349*, 255–260; d) T. Lakko, L. King, P. Fraker, *J. Immunol. Methods* **2002**, *261*, 129–139.

- [40] For fluorescence Cd^{2+} sensors, see a) M. E. Huston, C. Engleman, A. W. Czarnik, *J. Am. Chem. Soc.* **1990**, *112*, 7054–7056; b) V. K. Gupta, P. Kumar, *Anal. Chim. Acta* **1999**, *389*, 205–212; c) M. B. Inoue, I. C. Muñoz, M. Inoue, Q. Fernando, *Inorg. Chim. Acta* **2000**, *300–302*, 206–211; d) L. Prodi, M. Montalti, N. Zaccheroni, J. S. Bradshaw, R. M. Izatt, P. B. Savage, *Tetrahedron Lett.* **2001**, *42*, 2941–2944; e) A. M. Costero, R. Andreu, E. Monrabal, R. Martínez-Máñez, F. Sancenón, J. Soto, *J. Chem. Soc. Dalton Trans.* **2002**, 1769–1775; f) A. M. Costero, S. Gil, J. Sanchis, S. Peransí, V. Sanz, J. A. G. Williams, *Tetrahedron* **2004**, *60*, 6327–6334; g) T. Gunnlaugsson, T. C. Lee, R. Parkesh, *Org. Lett.* **2003**, *5*, 4065–4068; h) T. Gunnlaugsson, T. C. Lee, R. Parkesh, *Tetrahedron* **2004**, *60*, 11239–11249.

Received: March 17, 2006
Published online: September 5, 2006